

Review

Remote Sensing of Riparian Ecosystems

Miloš Rusnák ^{1,*}, Tomáš Goga ¹, Lukáš Michaleje ¹, Monika Šulc Michalková ², Zdeněk Máčka ², László Bertalan ³ and Anna Kidová ¹

¹ Institute of Geography, Slovak Academy of Sciences, Štefánikova 49, 814 73 Bratislava, Slovakia; tomas.goga@savba.sk (T.G.); geoglumi@savba.sk (L.M.); geogkido@savba.sk (A.K.)

² Department of Geography, Faculty of Science, Masaryk University, Kotlářská 2, 611 37 Brno, Czech Republic; sulc@mail.muni.cz (M.Š.M.); macka@sci.muni.cz (Z.M.)

³ Department of Physical Geography and Geoinformatics, University of Debrecen, Egyetem tér 1, H-4032 Debrecen, Hungary; bertalan@science.unideb.hu

* Correspondence: geogmilo@savba.sk

Abstract: Riparian zones are dynamic ecosystems that form at the interface between the aquatic and terrestrial components of a landscape. They are shaped by complex interactions between the biophysical components of river systems, including hydrology, geomorphology, and vegetation. Remote sensing technology is a powerful tool useful for understanding riparian form, function, and change over time, as it allows for the continuous collection of geospatial data over large areas. This paper provides an overview of studies published from 1991 to 2021 that have used remote sensing techniques to map and understand the processes that shape riparian habitats and their ecological functions. In total, 257 articles were reviewed and organised into six main categories (physical channel properties; morphology and vegetation or field survey; canopy detection; application of vegetation and water indices; riparian vegetation; and fauna habitat assessment). The majority of studies used aerial RGB imagery for river reaches up to 100 km in length and Landsat satellite imagery for river reaches from 100 to 1,000 km in length. During the recent decade, UAVs (unmanned aerial vehicles) have been widely used for low-cost monitoring and mapping of riverine and riparian environments. However, the transfer of RS data to managers and stakeholders for systematic monitoring as a source of decision making for and successful management of riparian zones remains one of the main challenges.

Keywords: riparian zone; vegetation; satellite; aerial images; lidar; UAV

Citation: Rusnák, M.; Goga, T.; Michaleje, L.; Šulc Michalková, M.; Máčka, Z.; Bertalan, L.; Kidová, A. Remote Sensing of Riparian Ecosystems. *Remote Sens.* **2022**, *14*, 2645. <https://doi.org/10.3390/rs14112645>

Academic Editor: Maria Laura Carranza

Received: 14 April 2022

Accepted: 29 May 2022

Published: 31 May 2022

Publisher's Note: MDPI stays neutral with regard to jurisdictional claims in published maps and institutional affiliations.



Copyright: © 2022 by the authors. Licensee MDPI, Basel, Switzerland. This article is an open access article distributed under the terms and conditions of the Creative Commons Attribution (CC BY) license (<https://creativecommons.org/licenses/by/4.0/>).

1. Introduction

Riparian zones are among the most biologically diverse and productive ecosystems on Earth. They are shaped by underlying physical processes associated with river flow, including erosion and deposition of sediment, periodic inundation, and groundwater-surface water exchange. In their natural state, riparian ecosystems are characterised by high spatial and temporal heterogeneity, which supports a diverse number of species, habitats, and ecological processes. Today, throughout most of the world, rivers and their riparian zones have been profoundly modified by human activities associated with river management (e.g., dams and flow regulation) and land-use pressures (e.g., agricultural conversion and irrigation withdrawals), altering the patterns and processes that sustain riparian functions and biodiversity [1–6]. The spatial delineation of riparian zones is mostly related to the streams and terrestrial landscapes that are affected by floods (as in the context of [7]) or on the vegetation cover along a river system (the edges of vegetation communities [8]) with the direct interactions between aquatic and terrestrial ecosystems [9].

Freshwater ecosystems are less resilient to negative impact caused by climate changes, direct human activities, or artificial demand for water resources. In the riparian

zone is a system adapted to close interactions of morphology, vegetation, and water flow in channels through which water forms, transforms, and reorganises fluvial systems in different spatial structures [10]. Anthropogenic modification, grade-control structures, and channelisation have resulted in the channel narrowing, transformation, and incision in many rivers worldwide [1,4,6,11–14]. Extraordinary floods and their geomorphological effectiveness are influenced by the actual state of the channel [15–17] and are related to the vegetation rejuvenation and direct channel modification. Feedback between flow, sediment dynamics, channel landforms, and riparian vegetation changes the riparian ecosystem in space and time. The fluvial geomorphic processes reciprocally interact with the riparian vegetation [18–21]. Feedback can ensure the functioning of fluvial ecosystems in terms of the transition from geomorphological instability (unstable bars with sparse vegetation) to geomorphological stability with lower biodiversity (dense willow cover) but higher productivity [18,22]. Riparian vegetation represents an important feature of it catching water, contributing to the strong resilience and resistance of plant and pioneer species. At the same time, it becomes a factor influencing biological diversity.

The monitoring of riparian ecosystems is essential for understanding the way that systems respond to stressors and management outcomes. Intensive field sampling can provide useful insights into the status and trends of local systems. However, this approach can be labour-intensive and costly due to its dynamic nature, the large area monitored, and the relative inaccessibility of riparian ecosystems [23]. Remote sensing techniques provide a powerful tool for monitoring riparian zones over long durations and large areas. The Landsat programme that began in 1972 opened up a wide range of uses for satellite data in the evaluation of landscape changes as well as in river research [24]. Improved satellite data resolution, increased number of revisit times, better spectral resolution, improved properties of sensors (both satellite and airborne), more developed passive scanning techniques (e.g., radar and lidar), and the innovation of modern field mapping technologies (echo sounding, drones, and terrestrial laser scanners) have allowed for detailed research into the dynamic interactions within riparian ecosystems [24].

The main challenge in remote sensing is capturing the different attributes or parameters that shape the riparian ecosystem. This includes understanding the physical factors and morphology of the channel, the flow parameters (velocity and temperature), the riparian vegetation, and the way individuals and populations mutually interconnect with processes [25]. Some clear advantages of remote sensing for assessing freshwater biophysical properties are the cost, the product accuracy, the data continuity, and the availability of programming software or personnel skills [23]. Remote sensing data are optimal for classifying or evaluating objects [26,27] and for estimating biophysical properties based on the algorithms linked to the spectral or intensity properties of a plant canopy, species composition [28], phenology [29], chlorophyll contents [30,31], water depth [32], sediment concentration and load, and amount of algae [33]. The physical properties reflected in the river morphology are key drivers affecting the topographical diversity, moisture gradients, and microhabitats [25]. The landform structure, substrate grain size and stratigraphy, geochemical properties, and water availability create the basic framework for riparian plant communities. Along with the flow regime and riparian vegetation, these parameters are essential for understanding the processes and interactions within the riparian landscape. Remote sensing offers efficient monitoring and detection of these three main riparian elements.

The objectives of this paper were (i) to provide a comprehensive overview of the published literature that has used remote sensing techniques to study riparian ecosystems; (ii) to describe the current state of applications of remote sensing in river research; and (iii) to identify the possible gaps to future research.

2. Database Processing

We understand the riparian ecosystem as a complex system including physical habitat parameters, the flow regime, and biota. Fluvial interactions are key elements of

this system and are defined based on the functional and structural properties *sensu* Dufour et al. [34]. A systematic review was carried out by making structured queries in the WOS (<http://apps.webofknowledge.com>, accessed on 9 June 2021) portal according to the PRISMA protocols and workflow diagram (Figure 1). A combination of quantitative and qualitative approaches was used based on the topic search (TS) and individual assessments of all articles from the search queries [35]. For the analyses, we created a list of specific terms and their synonyms for three main groups:

- The first group included articles related to the riparian ecosystem: “riparia*”, “floodplain*”, “ecosys*”, “vegeta*”, “change”, “success*”, “biogeo*”, and “ecol*”.
- The second group focused on river system specification: “river*”, “channel*”, “fluvial*”, “hydromorph*”, “hydro*”, “planform*”, and “morpho*”. To refine the results, we used the operation NOT with topics such as “estuary” OR “coast” to focus primarily on river systems.
- The third group was related to the remote sensing methods used in the article. In this case, we separated four basic types of sensors: (A) satellites, “satellite*”, “remote*”, “Landsat”, “sentinel”, and “image*”; (B) aerial images, “remote*”, “aerial*”, “photogra*”, and “image*”; (C) UAVs (unmanned aerial vehicles), “uav”, “drone*”, “uas”, “SfM”, “*motion”, and “raps”; and (D) airborne lidars (“lidar*”), with the NOT operator and the other word groups used to decrease noise within the search.

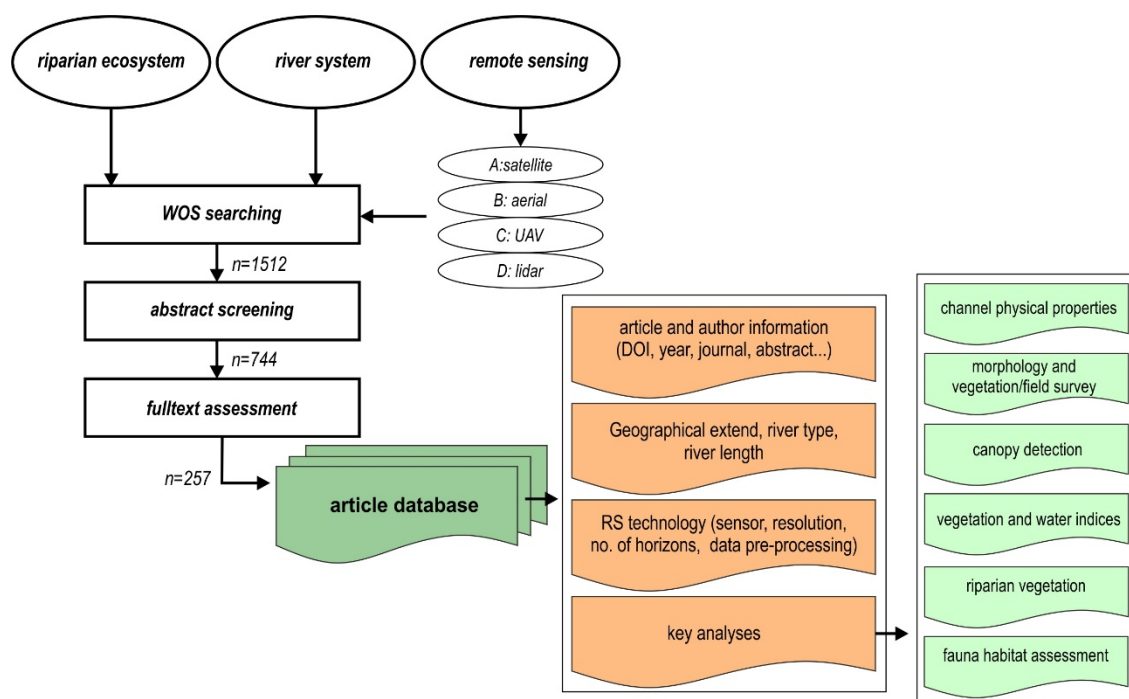


Figure 1. Workflow diagram of article extraction from the WOS database and article analyses.

The final query combined words from groups one and two and one of the sensor types (A–D) with the AND operator. The search was conducted in June 2021, and overall, 1512 articles were found in the first iteration. After the abstracts were screened in WOS and the studies that were not relevant to the aims of this study were excluded, 744 papers were downloaded for manual processing. In the last iteration, we analysed 257 papers. Any articles investigating freshwater wetlands, coastal areas, or LCs on the catchment scale (not related to river research) were excluded from processing. These 257 articles were subjected to a deep-content expert analysis to answer the main research questions. The database of processed articles thus included the primary bibliographic information exported from WOS (authors, article title, volume, issue, DOI, and abstract) and the main characteristics extracted from the content analyses (remote sensor type (A–D), country,

study area (km²/km), river name, planform, category, sensor type, horizons, resolution, number of horizons, study aim, data pre-processing, RS data analyses, classification parameters, field research, research related to hydrology, research related to morphology, research related to floodplain, ecology, or ecosystem, key analyses, and main results).

The quantitative analyses of the article abstracts were performed using elementary text mining methods implemented in the *tm* package [36]. All 257 analysed abstracts were imported into a text document, denoted as the corpus. Several pre-processing methods were applied for cleaning up and structuring the input text such as whitespace elimination, lower-case conversion, stop word removal, and number and punctuation removal. While the stemming process was not applied, lemmatisation was performed using the *textstem* package with the function *lemmatize_strings*. This process reduces a word to its base form through morphological analysis.

Count-based evaluation or term frequency analysis is one of the simplest methods used in text mining. Those terms have the highest frequencies of occurrence and thus should be rated as the most important. The results obtained using this approach can be easily interpreted and attractively visualised (e.g., using word clouds), while the process is computationally inexpensive [36]. An essential input for this analysis is the term-document matrix (Document Term Matrix (DoTeMa)). DoTeMa uses the bag-of-words modelling assumption, in which the frequency of terms occurring is more important than their order and structure. DoTeMa can be easily transformed into a data framework that can be visualised and directly interpreted, emphasising the research objective [36].

As follows from the above, the term frequency analysis does not take into account the importance of a term. This means that a more sophisticated text mining method should be applied, such as weighting. The most popular weighting approach is a method called *term frequency-inverse document frequency* (tf-idf), which reduces the impact of irrelevant terms and highlights discriminative ones by normalising each matrix element when taking into consideration the number of total documents [36]. Tf-idf combines a local weighting method—*term frequency*—with a global weighting method—*inverse document frequency*—with high values suggesting that a term occurs many times in a few documents and low values suggesting that a term occurs in all, most, or many documents [37]. High values of tf-idf indicate which terms best characterise the topics discussed in the documents contained within the corpus.

3. Quantitative Analysis of the WOS Database

3.1. Search Results

In the recent decade, the increasing interest in river ecosystems has been evident (Figure 2). Improvements in sensor technologies are reflected in the growing number of publications discussing the application of RS found in the WOS database. Most studies are from the Northern Hemisphere, mainly from Europe (43%) and North America (31%). On the other half of the world, Asia and Australia represent 13% and 8% of these studies, respectively (Figure 3). This result highlights the lack of studies in South America and Africa, with only 4% and 2% of the total number of studies, respectively, and with these studies focusing on the tropical forest ecosystem rather than a relationship with river morphology.

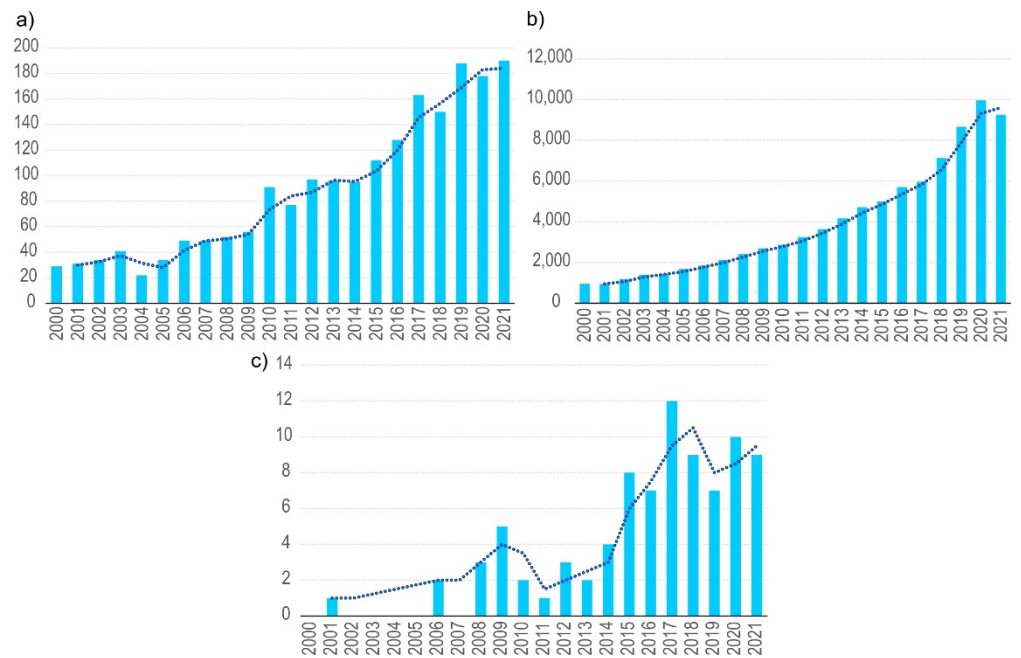


Figure 2. Number of articles in the WOS database over time for the topics (a) “riparian or river ecosystem”, (b) “remote sensing”, and (c) logical conjunction of both. Increases in the number of ES and RS topics are transformed into an increase in the use of RS in ecosystem research.

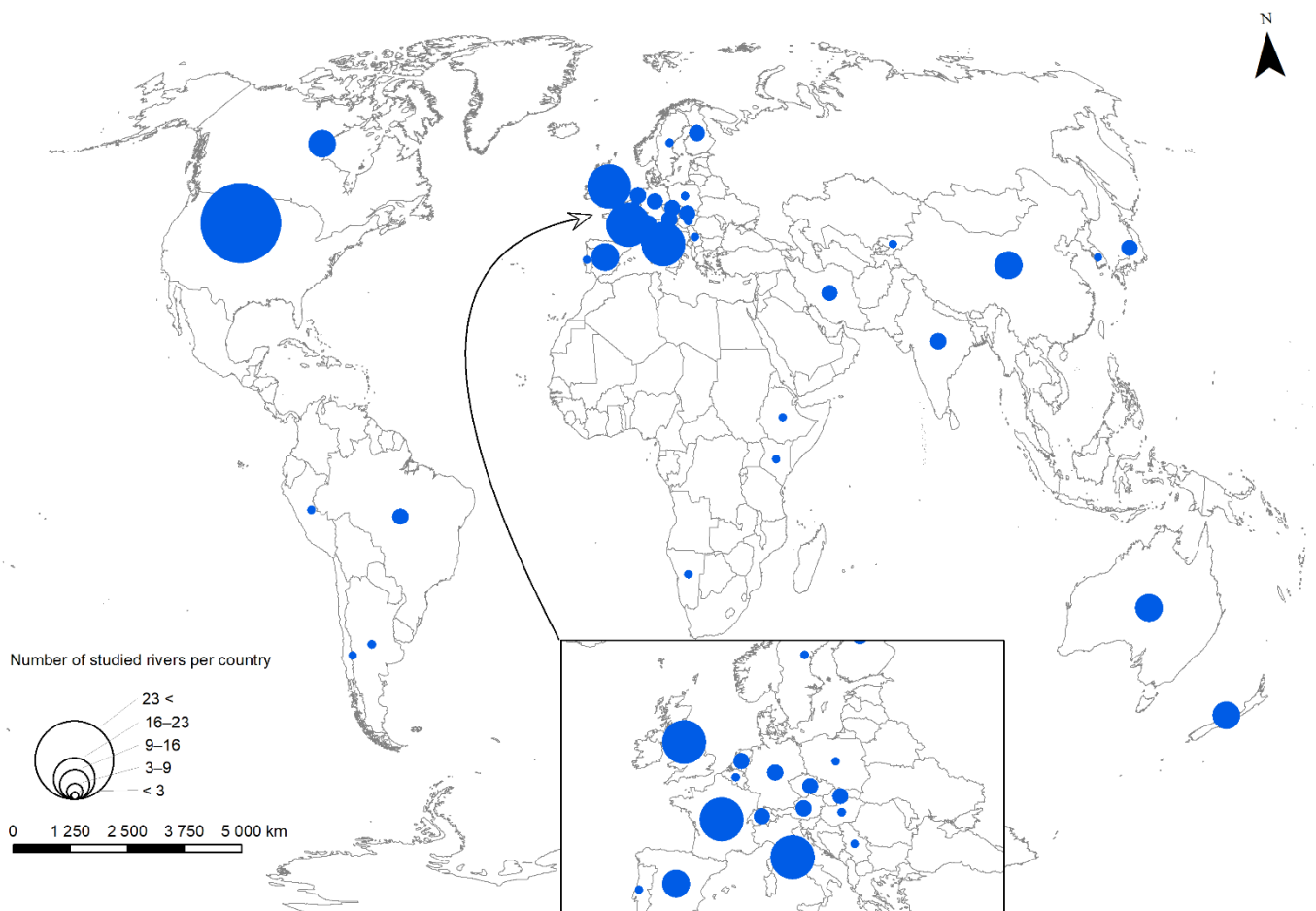


Figure 3. Locations of the areas studied as found from the WOS search.

Increasing availability of remote sensing technologies and software has led to the study of specific river research applications. RGB images with a resolution of approximately 1 m have been primarily used for river reaches up to 100 km long in the research of riparian ecosystems (Figure 4). A second large group of articles has used data from Landsat satellites with 30 m resolution and has focused on river lengths from 100 to 1000 km. Aerial images and Landsat data are the primary sources used for a detailed understanding of riparian ecosystems. Most of the articles did not address the river planform type (45%) and were related to the application of new technologies, the impact of stressors (dams and droughts), or the ecology and physiology of vegetation. Furthermore, 33% of the articles focused on the meandering and braided river system, and research focused mainly on dynamic river systems with active gravel bars, lateral movements, and multiple channel systems.

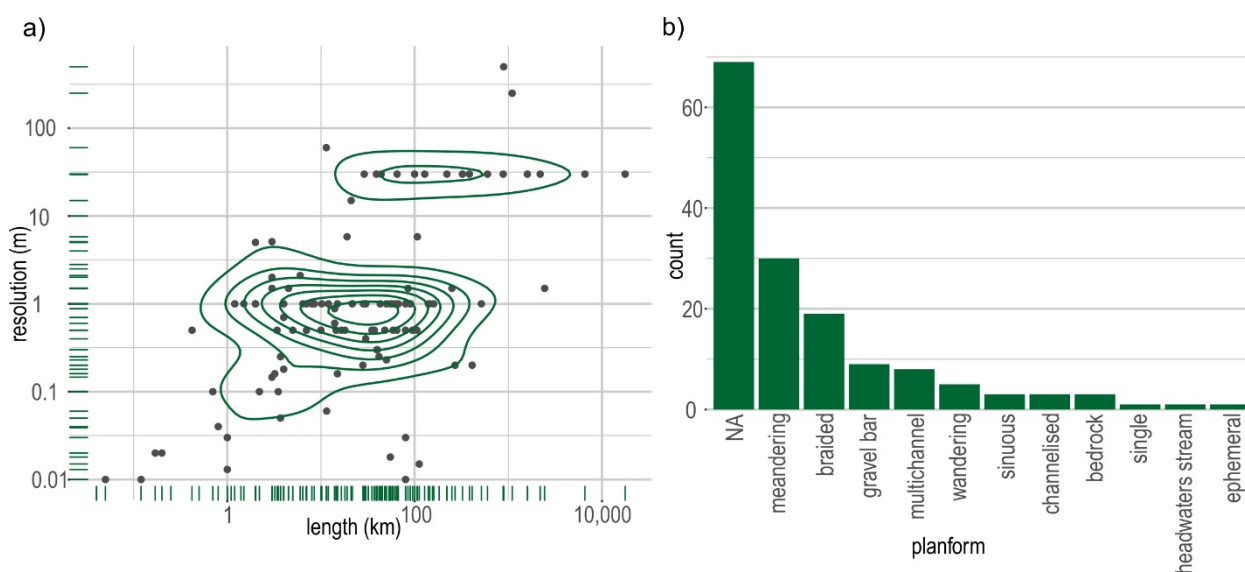


Figure 4. Relationship between sensor resolution and channel length (a) and a number of different river planforms (b) studied in the publications obtained from the WOS search. For most publications, the channel type was not explicitly mentioned and was marked as NA.

3.2. Abstract Term Analysis

A quantitative analysis was performed based on the frequency of terms and on word importance obtained from the abstracts included in the database of collected articles. The word cloud analyses (Figure 5a) pointed out that the terms “river” (890×) and “vegetation” (569×) dominated in terms of frequency. This finding is consistent with the research aims and is reflected by the study design and selected keywords during the WOS search. Some other prominent keywords included the fluvial system (riparian, channel, floodplain, flood, and flow), ecosystem management and vegetation (habitat, species, and forest), physiognomy (land, cover, and island), and morphology (bar). The tf-idf value (Figure 5b) was calculated for each term included in the primary corpus, which consisted of 257 abstracts with keywords such as “vegetation” (tf-idf = 3.04), “floodplain” (2.76), “riparian” (2.65), “flood” (2.34), “channel” (2.30), “change” (2.26), and “habitat” (2.17). The absence of the word “river” in the tf-idf analysis showed its obvious insignificance, while the highest tf-idf values obtained for specific terms showed that this corpus of the published literature is relevant, with an emphasis on the review objectives and PRISMA protocols.

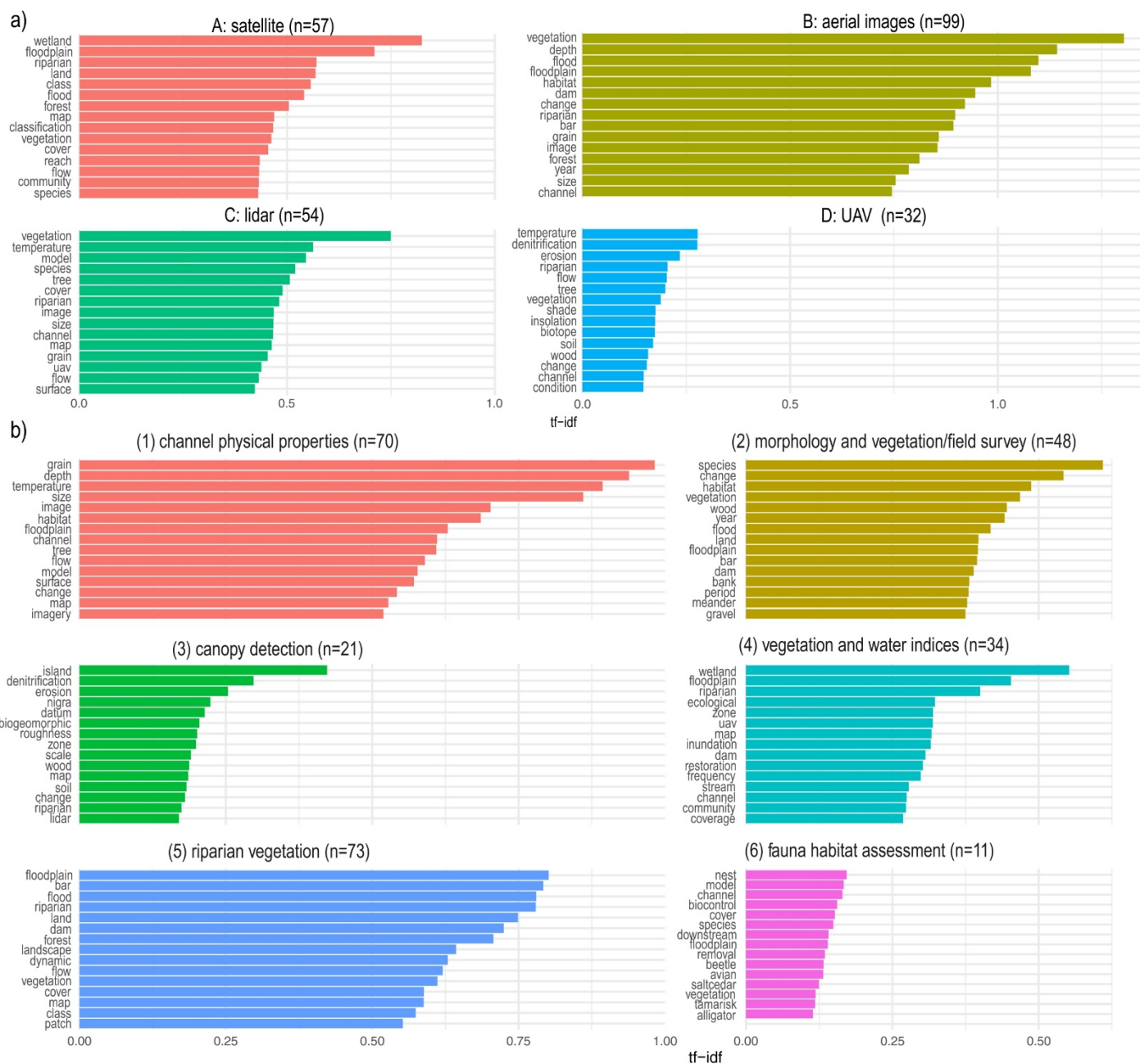


Figure 6. Word importance of the abstract clusters based on the tf-idf. Clusters were divided (a) into four main groups based on the types of remote sensing sensor and (b) the six main categories from the content analyses.

The word importance calculated within those clusters and the selected words proved the relevance of each cluster and their consistency. At this point, word importance verified all of the explanations specified in the individual sub-sections below.

4. Remote Sensing Application in River System Research

After compilation of the WOS database, main research trajectories were organised into six main categories: (i) physical channel properties; (ii) morphology and vegetation or field survey; (iii) canopy detection; (iv) application of vegetation and water indices; (v) riparian vegetation; and (vi) fauna habitat assessment.

4.1. Physical Properties of a River Channel Detected by Remote Sensing

The physical properties of a riparian zone create a baseline for ecosystem organisation along streams and lay out the requirements for survival, germination, succession of vegetation, and interactions between physical and biotic features. A number of remote sensing techniques have been used to identify the physical properties of river channels (Table 1). In general, the focus is primarily on identifying the properties of in-channel bed sediments (grain size), channel geometry and bed morphology (bathymetry), flow properties (velocity and temperature), and physical habitats. Grain size mapping uses two main approaches related to individual grain size measurements from the in situ methods described by Wolman (1954, [38]). The first approach uses the spatial and textural properties of images acquired by remote sensing surveys and the correlation among image properties with the field measurement (field grain size). In this case, the local spatial structures derived from the image texture are linked to the measured grain size [39–41]. The second approach uses UAVs in the application of a predictive calibration between the point cloud 3D properties (roughness) and measured grain size [42,43], formerly dominating terrestrial laser scanner (TLS) survey grain size detections. Due to the spatial resolution of the objects, aerial images and SfM photogrammetry data with resolutions of several centimetres are commonly used for grain size detection.

The subaerial in-channel topography is detected using the spectral-depth approach (optical bathymetry) or light refraction correction in through-water photogrammetry or SfM. The spectral properties are correlated with the empirical data. This approach is limited by the maximum detectable water depth and is affected by channel morphology, illuminations, and water turbidity, which have been studied in technical papers (see details in Table 1). Direct topography mapping of a submerged channel needs refraction correction based on the position and elevation of the water's edge [44] or using a multi-angle refraction correction of the 3D point clouds available such as python script `pyBathySfM v4.0` [45].

River flow monitoring is achieved through image velocimetry and particle identification for the tracking-phase movement. Previous methods developed for handheld cameras mounted on the bridges or riverbanks were combined with a drone planform for quick and safe methods of calculating discharge [46]. Temperature mapping of a river is focused on quantifying the spatiotemporal heterogeneity of temperature based on the acquisition of thermal infrared imagery (TIR) or using remote sensing data to extract tree cover data and a digital terrain model (DTM) or digital surface model (DSM) to simulate river temperatures (measure canopy opening and geomorphic data as an inputs for thermal modelling) or the effect of vegetation shadow on river temperature.

A complex approach for mapping physical channel properties can be used for the detection and mapping of in-channel physical habitats. The main physical river habitat parameters are constituted by the flow regime (hydraulics) and the physical template (fluvial sedimentology and geomorphology). Remote sensing is helpful in the direct classification of in-stream morpho-hydraulic habitats (e.g., glides, riffles, pools, and deep water eddy drop zones [47–49]); surface flow types (SFTs [50]); substrate sediment [51]; a combination of the morpho-hydraulic unit and vegetation (trees, vegetated bar, vegetated bank, submerged vegetation, emergent vegetation, and grass [52]); a combination of substrate sediment grain size and vegetation [53]; or a combination of all three (hydraulic habitats, sediment, and vegetation [54]). Supervised classification methods (maximum likelihood classification (MLC) and artificial neural networks (ANNs)) and manual habitat delimitation have been used in such a classification. Another approach applies a combination of RS capabilities for detecting channel morphology and bathymetry using hydrodynamic modelling (velocity distribution) for the classification of aquatic habitats (including bathymetry, river hydraulic, grain sizes, undercut banks, vegetation, and large wood [55,56]). A detailed review measuring the properties of a biophysical freshwater ecosystem can be found in Hestir et al. [23], which focused primarily on hyperspectral data and aimed to analyse freshwater wetlands (not river channels).

Table 1. Physical properties of river channel detected by remote sensing. Studies are sorted based on a short description of the methodologies and sensors used.

Feature	Description	Sensor (Data)	References
Grain size	Detecting the textural variations (image semivariance, entropy) and optical granulometry	Aerial images/non-metric camera from helicopter survey	[39–41,57]
		Hyperspectral images	[58]
		UAV (digital camera)	[59–61]
	Point cloud properties (roughness) related to grain size	UAV (digital camera)	[42,43]
Bathymetry	Optical bathymetry: channel topography	Satellite (WorldView-2)	[62]
		Multispectral/hyperspectral	[27,63,64]
		Aerial images/non-metric camera	[65–68]
		UAV (digital camera)	[69–72]
	Optical bathymetry: sensor comparison	Multispectral WorldView-3, Airborne hyperspectral CASI, UAS-based hyperspectral, Bathymetric LiDAR	[73]
	Optical bathymetry: absence of field data	Satellite (WorldView-2)/aerial images	[74,75]
	Optical bathymetry: effect of morphology	Hyperspectral	[76]
	Optical bathymetry: depth-reflectance relations	Hyperspectral	[77]
	Optical bathymetry: illumination correction	Aerial non-metric camera	[78]
	Optical bathymetry: field sampling distribution	Hyperspectral	[79]
Surface flow velocity	Application of image velocimetry algorithms for flow velocity detection	Aerial images	[80,81]
		UAV	[44,45,82,83]
River temperature	River temperature mapping	UAV and thermal imaging camera	[91–93]
	Data for a river temperature model	UAV and thermal imaging camera	[94–96]
		Aerial lidar	[97]
	Riparian shading on direct and diffuse solar radiation	Aerial lidar	[98–100]
Habitat mapping	In-stream habitats classification and mapping	Hyperspectral/multispectral	[47–49,54]
		UAV	[50–53]
	Habitat conditions (stream condition index)	Lidar/multispectral	[101]
	DEM (bathymetry) and hydraulic modelling (velocity) for habitat detection	Hyperspectral	[55]
		UAV	[56,102]
Riparian zone morphology	Floodplain 3D	Lidar	[103–105]
		Aerial images	[106,107]

4.2. Floodplain and River Morphology Related to Vegetation and Field Survey

Floodplain and river channel morphology are closely related to vegetation development. Hicks et al. [108] used a combination of bathymetry and hydraulic modelling for the in-channel detection of physical habitats combined with topography data and floodplain vegetation classification. Airborne lidar data were used for detecting the microhabitat requirements, phytocoenological survey, and Ellenberg's indicator values [109], and aerial images were used to classify floodplain habitats based on land cover physiognomy (Table 2) and their long-term evolution in relation to changes in the river morphology (pattern).

From detailed aerial images based on supervised classification, individual large woody (LW) pieces can be identified as a polyline and the log jams of large woody debris (LWD) can be supported by ground truth survey [110,111].

Another approach uses remote sensing data combined with field surveys. Optical images have been used to classify vegetation (vegetation cover) and to identify geomorphic processes. These data have been supplemented by field vegetation surveys (vegetation variation and floristic composition) and soil sampling [112–114]. Vegetation transition was studied to assess the mutual relation between vegetation and channel dynamics (environmental controls). A different group of studies [115–119] has evaluated the impact of floods, drought, post-dam hydrology alteration, and river regulation on the patterns and processes of identifying vegetation (vegetation survey and morpho or vegetation spatial delineation using RS) or with forest canopy metrics [120].

A combination of object detection related to channel morphology and vegetation is used for understanding riparian zone evolution. Studies have focused on a comparison of the changes in the land cover categories (vegetation, agriculture, residential, water body, and bars) and meander parameters (width, sinuosity, radius, etc., [121–123]) on the transformation of riparian vegetation (vegetated or unvegetated, woody vegetation, vegetated islands, etc.) classified from RS in relation to in-channel geomorphic changes (active channel width, pattern changes, and bar transformation [124–127]) or floodplain age mapping [128]. Moreover, several studies have explored the morphology–vegetation relationships and the effect of floods and high-magnitude events [27,129–131] or post-dam hydrology alteration [132–134]. Marteau et al. [135] used UAVs to carry out effective river restoration measures by combining DEMs of difference (DoD) and orthophoto (MLC classification).

Satellite images are affected by a combination of hydrodynamics parameters in MLC classification and field surveys, with the information spectrally derived from RS to estimate the automated floodplain roughness [136].

Table 2. Detection and classification of river morphology and vegetation with a detailed field survey of vegetation and soil properties. Studies are sorted based on a short description of the methodologies and sensors used.

Feature	Description	Sensor (Data)	References
Floodplain habitat	Habitat detection (combined with LC classification, vegetation survey)	Lidar/multispectral	[108]
		Lidar	[109]
		Lidar/aerial	[137,138]
		Aerial images	[139–141]
LWD	LWD detection (related to the field survey, channel morphology or application of supervised classification)	Aerial images	[142]
		Aerial images/lidar	[110]
		UAV	[111,143]
Morphology and vegetation relationship + field data	Environmental controls on vegetation dynamics (relation morphology with vegetation survey and bed material sampling)	Aerial images	[112–114,144,145]
		Aerial images/UAV	[146]
		UAV (digital camera)	[30]

	Flow regime changes and flooding on vegetation dynamics (relation morphology with field survey)	Satellite	[118]
		Aerial images	[115–117,119,147]
	Environmental controls on vegetation dynamics (forest canopy metrics)	Aerial lidar	[120]
	River morphology (bar age, channel pattern) with vegetation classification	Satellite	[121,122,148]
		Aerial images	[123–128,149–154]
Morphology + vegetation detection and classification (LC)	Effect of floods on river morphology and vegetation	Aerial images	[27,130,131]
		UAV (digital camera)	[129]
	Effect of post-dam hydro alteration	Aerial images/satellite	[133]
		Aerial images	[132,134]
	River restoration	UAV (digital camera)	[135]
Floodplain roughness	Automated floodplain roughness parameterisation by assessing the vegetation spectral properties and field survey	Satellite (SPOT-5)	[136]

4.3. Canopy Detection from RS

Vegetation canopies within river zones have been studied by combining airborne laser scanning and photogrammetry from aerial images or UAVs. The ecological evolution and vegetation recruitment have been assessed based on the changes in vegetation patches [155–157]. A group of studies used canopy height models (CHMs) to explore the spatial distribution and dynamics of vegetation (Table 3). Vegetation dynamics are related to changes in the channel morphology and are defined based on the different successional stages of vegetation classified from a canopy. Tree height, growth rate, and morphology transformation from airborne laser scanning (ALS) data are combined with field surveys (stem diameter, age, density, species, height, etc.) for an investigation of the island's evolution [158–162], the requirements of different habitats, and the life history of riparian tree species such as *Alnus incana* (L.) and *Populus nigra* (L.) [163]. Corenblit et al. [164] used a set of four aerial images to calculate the CHMs from photogrammetric elevation models and to analyse its relationship with geomorphic and biological in situ variables. Some studies have determined the direct relationship between the properties of biophysical vegetation (field survey) and the CHM [165,166]. Field surveys and three different sensors (ALS (0.5–2.4 m pixels), QuickBird (2.4 m pixels), and SPOT-5 (10 m pixels)) were used by Johansen et al. [167] for riparian zone mapping for a stream length of 26,000 km in Australia.

Some other authors have used data from CHMs to classify vegetation based on the vegetation height [168,169], which is useful for vegetation and habitat mapping. Hortobágyi et al. [170] presented an approach for analysing past vegetation and morphology dynamics by combining historical aerial image stereophotogrammetry and Structure-from-Motion (SfM). ALS data have been applied in the floodplain roughness parameterisation, where spatially distributed canopy height (stage dependence of vegetated model) has been used in hydrodynamic modelling [171,172] or automated roughness parameterisation by fusing QuickBird satellite and ALS data to estimate plant density, crown diameters, tree height, stem diameter, crown base height, and leaf area index [173].

Table 3. Canopy height model (CHM) used for an assessment of the biophysical properties, relationship between the CHM and field surveys, vegetation classification, and roughness parametrisation. Studies are sorted based on a short description of the methodologies and sensors used.

Feature	Description	Sensor (Data)	References	
Canopy height model (CHM) generation	Relation of CHM (tree height), vegetation survey (species, density, and diameter), and channel morphology	Aerial lidar	[158,161,167,174–176]	
		Aerial images	[164]	
		Aerial lidar/aerial images	[160,162,163]	
		Aerial lidar/satellite images	[177]	
	Using CHM for vegetation classification	Direct relation CHM and biophysical properties of vegetation	Aerial images	[168]
			UAV (digital camera)	[169]
		Compare stereophotogrammetry and Structure-from-Motion (SfM) for CHM generation	Aerial images/UAV	[170]
CHM and floodplain roughness parameterisation (vegetation height)	Roughness impact in hydrodynamic modelling	Aerial lidar	[171,172]	
	Regression model for roughness from tree heights, spectral properties, and field survey	Multispectral/aerial lidar	[173,178]	
Vegetation and riverbank erosion	Generation of CHM and hydraulic modelling in HecRAS	Aerial lidar	[179]	

4.4. Application of Vegetation and Water Indices in Riparian Zone Assessment

Medium resolution satellite images (~10–15 m) with multispectral bands are preferred in the regional and large-scale riparian surveys and calculation of vegetation properties based on the spectral transformation of two or more bands. In the riparian zone, the normalised difference vegetation index (NDVI) is primarily associated with healthy green vegetation, and the normalised difference water index (NDWI) is primarily used to monitor changes in water content. In recent years, developments in UAV technology and low-cost multispectral sensors have enabled users to capture vegetation indices (VIs) and modified VIs (for use with RGB drone images) for effective drone monitoring [180,181]. Multiband indices are used for the classification and delineation of vegetation (see Table 4), where the NDVI and NDWI threshold for vegetation is applied, and water objects are delineated [182,183].

Spectral indices are used as a class parameter for supervised classification [184–187], as a predictor variable in the calculation of a fractional vegetation cover (FVC) model [188], or are combined with structural vegetation properties and species composition (field survey) for vegetation classification [189–191]. Moreover, if multitemporal vegetation cover is delineated, succession can be detected by calculating the gain or loss in the vegetation area [180,192,193].

Several other studies have used spectral indices to identify the impact of changes in the hydrology regime by damming on vegetation [181,194] or to quantify vegetation dynamics as a function of flooding [195–197]. Chen et al. [198] used NDWI to identify the frequency of floodplain inundations, and Marchetti et al. [199] evaluated the relationships between NDVI patterns and floodplain hydrogeomorphic features. Spectral indices highlight the vegetation properties as the photosynthetic activity or chlorophyll content. Spatial-temporal variations in the vegetation coverage and spectral properties (greenness) can be used to evaluate the ecological condition of riparian vegetation [200–203]. Güneralp et al. [204] estimated the above-ground biomass (AGB) on the meander bend using complex spectral information from the sensors SPOT 5 and Landsat ETM+,

and Fernandes et al., 2020 [205] estimated the carbon stock of a Mediterranean riparian forest based on UAV multispectral images. The NDVI with climate and field measured data (2000–2019) have been used for temporal and spatial variation of AGB and its response to climate change in the Tibetan Plateau [206,207]. Spectral indices can be used to explore changes in vegetation productivity (NDVI) during the monitoring of restoration projects [208,209], during the identification of vegetation responses to shifting management [210], or in the assessment of green infrastructure [211].

Table 4. Vegetation properties and water area detection based on vegetation and water indices calculated from multispectral sensors. Studies are sorted based on a short description of the methodologies and sensors used.

Feature	Description	Sensor (Data)	References
Vegetation and LC classification	Identification of vegetation cover and LC classification	Satellite	[182–185,187,212]
	Combination of vegetation indices and Field survey (biophysical parameters) for model parametrisation and vegetation classification	Satellite + UAV	[186,188]
		Satellite + lidar	[189]
	Vegetation classification and succession phase assessment	Satellite	[190,191]
Vegetation impact to changes in hydrology regime	Vegetation classification and effect of hydrology alterations (damming)	Satellite	[192,193]
		UAV	[180]
	Relationships between NDVI and the groundwater depth	Satellite	[194]
	Floodplain LC and inundation frequency	Satellite + UAV	[181]
Inundation detection	Inundated areas by classification images based on the water area frequency (WAF) index	Satellite	[213]
		Satellite	[195–197]
Hydrogeomorphic dynamics	Relationship between NDVI patterns and floodplain dynamics	Satellite	[198]
Ecological indicators	Assessment ecological condition of riparian zone based on VI	Satellite	[199]
Biomass	Mapping of aboveground biomass carbon stock estimations	Satellite	[200–203]
		UAV (multispectral images)	[204,206,207]
Restoration	Using VI for restoration monitoring	Satellite	[205]
		UAV (digital camera)	[208]
Management	Vegetation (VI) response to shifting management activities	Satellite	[209]
			[210,211]

4.5. Riparian Vegetation Analyses and Assessment

Woody riparian vegetation is the most important element interacting with physical in-channel properties (sediment transport), channel morphology dynamics (erosion and deposition processes), and flow regime. Remote sensing provides continual datasets that facilitate the identification of spatial coverage and structural complexity of vegetation and its functions [214]. For an understanding and assessment of the vegetation habitat dynamics, land cover is used as a proxy, where land cover classes are detected and represent ecological habitats or process-oriented structures. Many authors have applied different methods of vegetation classification based on the physiognomic and texture patterns of a riparian landscape (Table 5). For vegetation detection, a general classification scheme is used, with vegetation as one feature of the riparian zone, broken down into

forest and grass classes. Some authors have used visual photointerpretation [215–219] of riparian land cover and categorized features into basic textural classes (channel and water, bar and sediments, settlement, forest, shrubland, grassland, and farmland). Hooke and Chen [220] mapped a complex system of woody vegetation in riparian areas with detailed successional stages of vegetation classification: shrub and herbs; juvenile sparse woodland; juvenile dense woodland; mature, sparse woodland; mature, dense woodland; old woodland; bank trees; and linear vegetation. Other authors have detected three main categories [26,221]: water, vegetation, and gravel by supervised classification (with main classification algorithms: maximum likelihood classification (MLC), random forest (RF), or convolutional neural network (CNN)). Vegetation land cover approaches have been used to detect the effects of flood events based on LC changes [222] and a combination of historical time-series for tracing the coevolution of river channels and riparian forests, and for investigation of the negative impact of human manipulation on river flow by post-dam hydrology alteration [223–226]. Furthermore, human disturbances and pressures in floodplain embankment and catchment land-use transformation over the last 50–60 years have been detected [227–230]. If the LC classification is applied, calculations of the landscape metrics are used to identify spatiotemporal land cover changes and variations in the riverscape patterns [231–234]. Dufour et al. [235] identified homogeneous vegetation units based on object-oriented aerial image classification (eight horizons), floristic composition, physiognomic parameters, and censused species and described landscape pattern dynamics based on landscape metrics. Morphological and vegetation responses mapped from land-cover changes are used to establish spatial priorities for conservation, restoration assessments, or its functional links with freshwater ecological status (Table 5).

A dynamic series of RS data was used to understand the process of vegetation succession and to identify the spatiotemporal trajectories of vegetation patches in different successional phases. Previous work has identified physical and biological processes governing the establishment of vegetation by manual digitalisation of vegetation classes [236–241], object-based semi-automated vegetation classification [242], or random forest classifier algorithm (29 detailed land cover classes, [243]) and related its spatial changes to channel morphology changes (ecotope transition from succession to rejuvenation or stability). Vautier et al. [244] used spatiotemporal stereophotogrammetric analyses of the CHM to identify geomorphic, pioneer, and biogeomorphic phases based on the vegetation heights. Tree ring analysis [245,246] with remote sensing land-cover delineation has been used for the early successional stages of woody vegetation detection on the surrounding gravel bar, and landscape metrics (Shannon diversity, dominance, fragmentation, patch metrics, and edge density) have been applied for assessments of the landscape habitat turnover [247–249]. A spatial aspect of sediment deposition, erosion, and vegetation colonisation (fine-scale vegetation encroachment) has been examined in several studies based on the detection of vegetation patches [155,250,251].

The mapping of riparian woody species in the riparian zone is necessary for understanding the cause-and-effect relationships between the vegetation community and channel and floodplain morphology, where individuals start from the germinant seedling stage and grow into the juvenile stage. RGB data prevail in the manual interpretation of areal extent, structure, and species composition [252–255], and multispectral and hyperspectral data prevail for semi- and automatic classification [256–260] on the different levels of plant composition (individuals, populations, and community).

A specific application is mapping riparian invasive taxa as a critical task for management and its threat to the ecosystem. Michez et al. [261] identified patches of invasive species from UAV orthophotos based on object classification (RF classification in eCognition). The spectral–structural workflow for classifying invasive species was developed using UAV multispectral data (combination of NDVI, NDWI, soil-adjusted vegetation index (SAVI), normalized difference snow index (NDSI), enhanced vegetation index (EVI-2), green normalized difference vegetation index (GNDVI), RGB, near-infrared

(NIR), and red edge (RE)) combined with the CHM model from SfM algorithms and field surveys [262]. Aerial multispectral data were used for the classification of Tamarisk (*Tamarix* spp.) and greenness calculated from the NDVI for an assessment of a beetle-impacted Tamarisk area [263]. The effects of flow regime on manually digitised floodplain invasive vegetation based on 67 flow metrics (indicators of hydrologic alteration and environmental flow components) have been studied on the 1.1 km long reach of the Ahuriri River [264,265].

A sub-decimetres resolution of UAV images has allowed for the classification of aquatic macrophytes (*Eichhornia crassipes* and *Phragmites australis*) [266,267] or green algae (*Cladophora glomerata*) [33], where the authors have emphasised the importance of lightweight and rapid response aerial imaging systems for quick and low-cost monitoring.

Table 5. Vegetation detection, successional phase identification, and individual species population classification in the riparian zone. Studies are sorted based on a short description of the methodologies and sensors used.

Feature	Description	Sensor (Data)	References
Riparian vegetation detection	LC and vegetation classification in the riparian zone	Satellite	[216,219]
		Aerial images/(satellite)	[218]
		Aerial images	[215,217,220,268]
		UAV (multispectral/digital camera)	[26,221,269]
	Effect of floods on the vegetation LC and vegetation recruitment	Satellite	[222]
	Effect of damming on the vegetation LC	Satellite	[226]
		Aerial images	[223–225]
	Disturbances and pressures on the vegetation LC	Aerial images	[227,229,230]
		Google Earth images	[228]
	Changes in vegetation LC and landscape metrics calculation	Satellite	[231–233]
		Aerial images	[234,235,270]
	Vegetation LC for ecological indicators assessment	Satellite	[271,272]
		Aerial images	[273]
	Structure of LC for management plans	Satellite	[274]
		Aerial images	[275–277]
	Vegetation dynamics simulation	Aerial images	[278]
Vegetation variable from field survey and RS data	Multispectral	[279]	
Vegetation succession	Biogeomorphic succession supported with vegetation survey (dendrochronology)	Aerial images	[245,246]
		Satellite	[243,280]
	Vegetation phase dynamics for identification of vegetation establishment (biogeomorphic phases)	Aerial images/satellite	[237,241]
		Aerial images	[236,239,242,281]
		Aerial images/lidar	[244,282]
	Biogeomorphic phases detection and landscape metrics	UAV (digital camera)	[240]
		Aerial images	[247–249]
	Vegetation colonisation and encroachment	Aerial images	[155,250]
Multispectral/lidar		[283]	
UAV (digital camera)		[251]	
Manual classification of riparian vegetation	Aerial images/satellite	[252,284]	
	Aerial images	[254,255]	

Vegetation communities/species classification	Unsupervised (ISODATA) classification of riparian vegetation	UAV (digital camera)	[253]
		Hyperspectral/lidar	[256]
	Supervised classification	Satellite	[257,259,260]
		Hyperspectral	[258]
Invasive riparian vegetation	Manual classification	Satellite/aerial non-metric camera	[285]
		Aerial images	[264,265]
	Supervised classification	Multispectral	[263]
		UAV (RGB, multispectral camera)	[261,262]
Aquatic vegetation	Manual classification	UAV (digital camera)	[266,267]
	supervised classification	UAV (digital camera)	[33]

4.6. Fauna Habitat Assessment in the Riparian Zone

Assessments of wildlife habitat status are required to successfully implement restoration projects as well as to successfully manage perspectives. The landscape properties detected from RS data create a proxy for fish habitat assessment or predictive animal models (abundance, preference, and suitability) in different riparian zones [286,287]. Fauna abundance and distribution depend on the in-channel and floodplain morphology, water depth, bed material, woody debris accumulation, bank vegetation, and floodplain vegetation composition (Table 6). Remote sensing data were used for detecting the riparian zone land cover based on water class and vegetation and for creating relationships between the field physical metrics and parameters derived from satellite data [288]. Other authors focused primarily on manual in-channel habitat classification from RS (pool-riffles, bed material, and flow properties) as a potential fish habitat [289] and its changes due to vegetation removal [290] or to identify parameters (geomorphic and potential fish habitat variables) for calculating the habitat richness index [287].

Arantes et al. [291] and Mollet et al. [292] combined in situ fish habitat data, environmental data, and landscape structures mapped from satellites for the identification of habitat preferences and to assess habitat conditions. Moreover, some studies focused on the identification of the habitat suitability index for alligators [293], on ground nest probability and its reflections in environmental constraints [294] and the application of vegetation indices (NDVI, EVI, and EVI2) from multispectral images as a predictor for insect habitats [295,296], or on avian abundance [297].

Table 6. Wildlife habitat status assessment using RS technologies. Studies are sorted based on a short description of the methodologies and sensors used.

Feature	Description	Sensor (Data)	References
Fish habitat detection	Habitat complexity assessment and distribution	Satellite	[288]
		Aerial images	[287,289,290]
		Aerial lidar	[286]
Habitat sustainability	Fish habitat preference	Satellite	[291]
		Satellite/lidar	[292]
	Suitability index for alligator/caiman	Satellite	[294]
		Satellite/lidar	[293]
	Insect habitat prediction based on VI	Satellite	[295,296]
	Predictive models for avian abundance and species richness	Satellite	[297]

5. Remote Sensing in the Riparian Zone: Global Challenges and Opportunities

This review analysed 257 studies and pointed out the wide range of uses for remote sensing in riparian ecosystem research, with focuses on ecological functioning and dynamic interactions between biota and the fluvial landscape. The aerial and satellite imagery are widely used in fluvial geomorphology for the identification in-channel planform and morphological changes [298–301]. Based on the study objectives, these areas were excluded from our evaluation but still present an extensive field of RS applications in the long-term evaluation of river trajectories. The advancement in sensors, platforms, and software innovation may facilitate the adoption of RS technology for effective and less time-consuming research and monitoring of rivers.

Multiple uses of the different sensor combinations and interconnections between scientific disciplines led to problems with categorising of selected papers into several research groups. Therefore, a subjective approach was applied to include these articles into the six main categories using expert and text mining content analyses. Potential limitations are related to the selection of the research query samples and topics that reflected the database creation process, e.g., selected specific terms and synonyms for main groups. The issue arose from detailed analyses of the result wherein the third group focused on basic sensor types and did not include satellites with very high resolution (e.g., Skysat, Pleiades). This could be result of search query composition or content analyses (these types were not used in riparian ecosystem research within our specific groups). Moreover, the selection of the articles was limited. Only papers published to June 2021 and in the WOS database were incorporated into analyses. During the quantitative text mining, a total of 4586 unique terms were used after pre-processing. Despite a relatively high number of analysed articles (257), only terms included within abstracts were used and a relatively low number of non-sparse entries (27,565/1,141,865), which resulted in a sparsity of 98%. Full-text quantitative text analysis should be considered as the next step for detailed, unsupervised clustering and more precise quantitative analysis. Further, user-based clustering (used in this paper) is subject to a high risk of expert malignancy and also, this process is time consuming and requires a high level of expertise.

However, riparian ecosystem scientists still need to face the challenge of monitoring the evolution of river zones and assessment of ecosystem functions. Current limited knowledge of the riparian zones' evolution requires new analytical tools for inferring past evolutions that are essential for predicting future trajectories and for understanding the complexity of river systems [302]. From the literature review and state-of-the-art RS applications in riparian ecosystem research, several main challenges could be addressed:

- Knowledge transfer between the evolution of remote sensing processing and river scientists or managers;
- The technical availability of user-friendly methods and its routine application in river research;
- The effectiveness of RS techniques for information mining;
- The transfer of pixel data to processes and the integration of quantitative and qualitative information;
- Near real-time monitoring;
- Data mining;
- Open data repositories and policies.

An interdisciplinary approach is necessary for understanding riparian zone systems and the complex responses caused by multiple agents. Knowledge transfer from a technical background and RS data processing to river research and management are highly important. Moreover, precise monitoring and data mining are required. Huylenbroeck et al. [214] emphasised the mutual benefits for managers (e.g., ecologists, hydrologists, and geomorphologist) and remote sensing experts and pointed out that developments in technology often precede application in real-field situations. An example is the application of UAVs for detailed topography mapping in which Structure-from-

Motion (SfM) emerged as a flexible and operational method [303] that allows many users without formal training and knowledge of the correct methodologies to apply this method for topography modelling while mitigating systematic errors, uncertainty, and independent quality assurance measurements [85,304,305]. Systematic monitoring and detailed analyses combined with empirical and field research create important sources for decision making and the successful management of riparian zones and river restoration. Benefits of detailed RS data such as quantitative assessments and modelling outweigh more traditional decision-making processes, which often lack the quantification and requirements for formalisation and operationalisation.

Analyses of 257 articles pointed to the different utilisation of the RS data, where their application enables substitute intensive fieldwork collection (low-density data coverage) with the continuous dataset for identification of physical channel properties, water flow parameters, or vegetation attributes. In some cases, they are applied as a complementary tool for field mapping (e.g., depth [27], floodplain DEM [109], changes of channel environmental properties [112–114,144,145], or vegetation parameters from the CHM [165,166]). RS data are mostly used for direct object detection and quantifying object parameters. Based on our analyses, vegetation (together with channel morphology) was the main object extracted from RS in the riparian ecosystem by analyses of the spatial extent or land cover changes [216,219]. Vegetation objects were often linked with the assessment of the external impacts that led to ecosystem transformation (flood [222], damming [273], and catchment-scale management [275–277]) and were analysed by using the spectral transformation of two or more bands to indices [184–187], lidar data, sensor combination, or detailed mapping and monitoring of the species composition [189–191]. Multitemporal data acquisition led to long-term change analyses and succession detection by identification of the gain or loss in the vegetation area [180,192,193]. Furthermore, riparian ecosystem transformation could be detected over the last 50–60 years [227–230], where could be integrated with data from historical aerial surveys, satellite data, and new technology such as is lidar or UAVs for conservation, restoration, and freshwater ecological status assessments. The significant group of the papers described and tested methodology for riparian ecosystem parameter extraction (e.g., channel depth [44,45,78] or grain size [39–41]) and object delineation (vegetation automatic classification [26], stereophotogrammetric analyses of historical data [244], or automatic classification of riparian woody species [257,259,260]). Appearance of user-friendly software applications (for SfM processing, orthorectification, correction, and classification) and open data repositories (e.g., Copernicus Open Access Hub and Earth Explorer) with pre-processed free temporal data [24,214] opens a new method of RS application in research of riparian ecosystems. These data can be processed with minor investments (open source software for monitoring and classifications based on spectral characteristics with object detections) or complemented with field data measurements and surveys (canopy properties, vegetation health status, or image texture granulometry determination). In recent years, we have witnessed the progress in the development of open-access toolboxes incorporated into commercial or open-access GIS solutions [306], such as Fluvial-Corridor-Toolbox-ArcGIS [307], River Bathymetry Toolkit [308], Geomorphic Change Detection [309], BASEGRAIN (<https://basement.ethz.ch/download/tools/basegrain.html>, accessed on 17 February 2022), and GRAINet [59].

The application of RS is time-effective and cost-effective; therefore, accuracy and uncertainty must be considered. Application of RS still focuses mainly on the local or regional scale and on the reach segment. The historical archive of RS data enables insight into past and back processing of historic datasets for new emerging scientific applications; diachronic analyses for past process detection and scaling actual models; and predicting future development. A retrospective reassessment of the hypotheses of landscape evolution and processes is also necessary [310].

RS technology enables the creation of spatially representative information stored in pixels or a XY(Z) point system. For process-oriented applications, reducing information

to methodologically effective descriptions of objects is essential. The surface of the Earth and vegetation properties are reduced to homogeneous riparian objects represented by statistically processed spectral, elevation, geometric, or morphometric characteristics. The detection of river system objects based on the identification of processes can be used to apply such procedures automatically to assess their variability, associated ecological integrity, and the diversity of the system. The transfer of point-based quantitative information to analytical and qualitative structures such as habitats and processes still remains a challenge. At the same time, spatial referenced data enable evaluation of the spatial context and conduction of the structured multi-scale analyses. A new technique for analysing images has arisen by applying “big data” processing and artificial intelligence (AI, machine learning, and convolutional neural networks) to object detection, analytical assessments, and riparian zone process understanding [26]. Application of AI increases classification performance over 90% and makes it possible to increase detectable features in the riparian landscape, and as stated Carbonneau et al. [26], potentially enables using RGB images instead of multi- and hyperspectral sensors for high-accuracy classifications. At the same time, higher spatial and temporal resolutions enable transformation of river monitoring from irregular and traditional point mapping to continuous monitoring at any point in the riparian ecosystem.

A combination of methods for automated data processing and improvement of the big data infrastructure and computational power facilities provides the ability to conduct continual or near real-time environmental monitoring [24,306]. This challenge is now included at smaller scales for hydrologic monitoring (velocity measurement) or management activities related to restoration processes. Integration of multiple systems such as camera-based monitoring stations, surveys of surface hydrology, river channel morphology, and riparian vegetation structure and density conducted at near real-time could reveal their detailed interactions even on the catchment scales. The derived data could also serve as an important additional refinement for catchment-based hydrological modelling [311].

Tomsett et al. [24] proposed an open repository for sharing data and knowledge as an important tool for decision making and good-practice dissemination. To study riparian ecosystems effectively, support for planning and policy is important. Research findings and RS data are essential for combating unsustainable riparian ecosystem changes or transformations and should be included in policy making and its implementation. However, the transformation of real riverine processes to complex models and the conceptualisation of a complex landscape system with many drivers and connections are extremely difficult, and it is imperative to continue the development in RS practice. Therefore, anticipating solutions to future problems, thus helping to make interventions and providing resilience to future negative changes, is important.

6. Conclusions

In the recent decade, the number of new remote sensing methods and sensor development has led to its wide application in the riparian zone studies. The higher resolution and affordable price for technical equipment and software processing have allowed faster field data acquisition and processing, which have led to a more detailed understanding of the functioning of riparian zones while simultaneously reducing the amount of cost, time, and effort taken for processing. Additionally, the extensive coverage of publicly available satellite images (e.g., Sentinel and Landsat) gives a unique opportunity to study riparian zones all over the world in resolution that was not available ever before. This opportunity allows for researchers to study riparian zones both at the local and global scales.

The combination of sensor improvement and technical availability contribute to increasing the use of remote sensing for detailed analyses and monitoring of in-channel processes, morphology of rivers, vegetation properties, floods, and river-floodplain connections. Together with the improvement of drones, equipped with different types of

sensors, they accelerate field data acquisition and information mining to transfer of pixels to process-oriented information. The comprehensive analysis of 257 articles that have used RS in riparian ecosystems pointed to main areas of application in the current state of its application that is linked with detecting physical channel properties, morphology, canopy and riparian vegetation changes, and habitats. The application of RS clearly shows potential for transfer of knowledge to local managers and stakeholders and for the successful management of riparian zones.

Author Contributions: Conceptualisation, M.R., A.K. and T.G.; methodology, M.R. and L.M.; formal analysis, M.R., L.M., M.Š.M., Z.M. and L.B.; data curation, M.R.; writing—original draft preparation, M.R.; writing—review and editing, Z.M., M.Š.M. and L.B.; visualisation, L.M. and T.G. All authors have read and agreed to the published version of the manuscript.

Funding: This research was funded by the Slovak Scientific Grant Agency VEGA under grant [2/0086/21], “Assessment of the impact of extreme hydrological phenomena on the landscape in the context of a changing climate”. LB was also supported by the Thematic Excellence Programme (TKP2020-NKA-04) of the Ministry for Innovation and Technology in Hungary.

Acknowledgments: We kindly thank Maciej Liro and Malia Volke for their comments and contributions during the preparation of this manuscript.

Conflicts of Interest: The authors declare no conflict of interest.

References

- Škarpich, V.; Hradecký, J.; Dušek, R. Complex transformation of the geomorphic regime of channels in the forefield of the Moravskoslezské Beskydy Mts.: Case study of the Morávka River (Czech Republic). *CATENA* **2013**, *111*, 25–40. <https://doi.org/10.1016/j.catena.2013.06.028>.
- Liébault, F.; Piégay, H. Causes of 20th century channel narrowing in mountain and piedmont rivers of southeastern France. *Earth Surf. Process. Landf.* **2002**, *27*, 425–444. <https://doi.org/10.1002/esp.328>.
- Scorpio, V.; Roszkopf, C.M. Channel adjustments in a Mediterranean river over the last 150 years in the context of anthropic and natural controls. *Geomorphology* **2016**, *275*, 90–104. <https://doi.org/10.1016/j.geomorph.2016.09.017>.
- Ziliani, L.; Surian, N. Evolutionary trajectory of channel morphology and controlling factors in a large gravel-bed river. *Geomorphology* **2012**, *173–174*, 104–117. <https://doi.org/10.1016/j.geomorph.2012.06.001>.
- Zawiejska, J.; Wyzga, B. Twentieth-century channel change on the Dunajec River, southern Poland: Patterns, causes and controls. *Geomorphology* **2010**, *117*, 234–246. <https://doi.org/10.1016/j.geomorph.2009.01.014>.
- Wyzga, B.; Zawiejska, J.; Radecki-Pawlik, A. Impact of channel incision on the hydraulics of flood flows: Examples from Polish Carpathian rivers. *Geomorphology* **2016**, *272*, 10–20. <https://doi.org/10.1016/j.geomorph.2015.05.017>.
- Naiman, R.J.; Décamps, H. The Ecology of Interfaces: Riparian Zones. *Annu. Rev. Ecol. Syst.* **1997**, *28*, 621–658. <https://doi.org/10.1146/annurev.ecolsys.28.1.621>.
- Naiman, R.J.; Décamps, H.; McClain, M.E.; Likens, G.E. *Riparia*; Elsevier: Amsterdam, The Netherlands, 2005; ISBN 9780126633153.
- Gregory, S.V.; Swanson, F.J.; McKee, W.A.; Cummins, K.W. An Ecosystem Perspective of Riparian Zones. *Bioscience* **1991**, *41*, 540–551. <https://doi.org/10.2307/1311607>.
- Brierley, G.J.; Fryirs, K.A. *Geomorphology and River Management*; Brierley, G.J., Fryirs, K.A., Eds.; Blackwell Publishing: Malden, MA, USA, 2004; ISBN 9780470751367.
- Scorpio, V.; Zen, S.; Bertoldi, W.; Surian, N.; Mastrorunzio, M.; Dai Prá, E.; Zolezzi, G.; Comiti, F. Channelization of a large Alpine river: What is left of its original morphodynamics? *Earth Surf. Process. Landf.* **2018**, *43*, 1044–1062. <https://doi.org/10.1002/esp.4303>.
- Rádoane, M.; Obreja, F.; Cristea, I.; Mihailă, D. Changes in the channel-bed level of the eastern Carpathian rivers: Climatic vs. human control over the last 50 years. *Geomorphology* **2013**, *193*, 91–111. <https://doi.org/10.1016/j.geomorph.2013.04.008>.
- Brierley, G.J.; Mum, C.P. European impacts on downstream sediment transfer and bank erosion in Cobargo catchment, New South Wales, Australia. *CATENA* **1997**, *31*, 119–136. [https://doi.org/10.1016/S0341-8162\(97\)00025-8](https://doi.org/10.1016/S0341-8162(97)00025-8).
- James, L.A. Channel incision on the Lower American River, California, from streamflow gage records. *Water Resour. Res.* **1997**, *33*, 485–490. <https://doi.org/10.1029/96WR03685>.
- Hooke, J.M. Variations in flood magnitude–effect relations and the implications for flood risk assessment and river management. *Geomorphology* **2015**, *251*, 91–107. <https://doi.org/10.1016/j.geomorph.2015.05.014>.
- Kijowska-Strugała, M.; Wiejaczka, Ł.; Gil, E.; Bochenek, W.; Kiszka, K. The impact of extreme hydro-meteorological events on the transformation of mountain river channels (Polish Flysch Carpathians). *Z. Für Geomorphol.* **2017**, *61*, 75–89. <https://doi.org/10.1127/zfg/2017/0434>.

17. Gorczyca, E.; Krzemień, K.; Wrońska-Wałach, D.; Sobucki, M. Channel Changes due to Extreme Rainfalls in the Polish Carpathians. In *Geomorphological Impacts of Extreme Weather*; Springer Netherlands: Dordrecht, Netherlands, 2013; pp. 23–35.
18. Bendix, J.; Hupp, C.R. Hydrological and geomorphological impacts on riparian plant communities. *Hydrol. Process.* **2000**, *14*, 2977–2990. [https://doi.org/10.1002/1099-1085\(200011/12\)14:16/17<2977::AID-HYP130>3.0.CO;2-4](https://doi.org/10.1002/1099-1085(200011/12)14:16/17<2977::AID-HYP130>3.0.CO;2-4).
19. Hupp, C.R.; Bornette, G. Vegetation as a Tool in the Interpretation of Fluvial Geomorphic Processes and Landforms in Humid Temperate Areas. In *Tools in Fluvial Geomorphology*; John Wiley & Sons, Ltd.: Chichester, UK, 2005; pp. 269–288, ISBN 9780470868331.
20. Parsons, M.; Thoms, M.C. Hierarchical patterns of physical–biological associations in river ecosystems. *Geomorphology* **2007**, *89*, 127–146. <https://doi.org/10.1016/J.GEOMORPH.2006.07.016>.
21. Francis, R.A.; Corenblit, D.; Edwards, P.J. Perspectives on biogeomorphology, ecosystem engineering and self-organisation in island-braided fluvial ecosystems. *Aquat. Sci.* **2009**, *71*, 290–304. <https://doi.org/10.1007/S00027-009-9182-6>.
22. Corenblit, D.; Steiger, J.; Gurnell, A.M.; Tabacchi, E.; Roques, L. Control of sediment dynamics by vegetation as a key function driving biogeomorphic succession within fluvial corridors. *Earth Surf. Process. Landf.* **2009**, *34*, 1790–1810. <https://doi.org/10.1002/esp.1876>.
23. Hestir, E.L.; Brando, V.E.; Bresciani, M.; Giardino, C.; Matta, E.; Villa, P.; Dekker, A.G. Measuring freshwater aquatic ecosystems: The need for a hyperspectral global mapping satellite mission. *Remote Sens. Environ.* **2015**, *167*, 181–195. <https://doi.org/10.1016/j.rse.2015.05.023>.
24. Tomsett, C.; Leyland, J. Remote sensing of river corridors: A review of current trends and future directions. *River Res. Appl.* **2019**, *35*, 779–803. <https://doi.org/10.1002/RRA.3479>.
25. Merritt, D.M.; Scott, M.L.; Leroy Poff, N.; Auble, G.T.; Lytle, D.A. Theory, methods and tools for determining environmental flows for riparian vegetation: Riparian vegetation-flow response guilds. *Freshw. Biol.* **2010**, *55*, 206–225. <https://doi.org/10.1111/j.1365-2427.2009.02206.x>.
26. Carbonneau, P.E.; Dugdale, S.J.; Breckon, T.P.; Dietrich, J.T.; Fonstad, M.A.; Miyamoto, H.; Woodget, A.S. Adopting deep learning methods for airborne RGB fluvial scene classification. *Remote Sens. Environ.* **2020**, *251*, 112107. <https://doi.org/10.1016/j.rse.2020.112107>.
27. Bryant, R.G.; Gilvear, D.J. Quantifying geomorphic and riparian land cover changes either side of a large flood event using airborne remote sensing: River Tay, Scotland. *Geomorphology* **1999**, *29*, 307–321. [https://doi.org/10.1016/S0169-555X\(99\)00023-9](https://doi.org/10.1016/S0169-555X(99)00023-9).
28. Hestir, E.L.; Greenberg, J.A.; Ustin, S.L. Classification trees for aquatic vegetation community prediction from imaging spectroscopy. *IEEE J. Sel. Top. Appl. Earth Obs. Remote Sens.* **2012**, *5*, 1572–1584. <https://doi.org/10.1109/JSTARS.2012.2200878>.
29. Notaro, M.; Emmett, K.; O’Leary, D. Spatio-temporal variability in remotely sensed vegetation greenness across Yellowstone National Park. *Remote Sens.* **2019**, *11*, 798. <https://doi.org/10.3390/rs11070798>.
30. Davis, J.; Blesius, L.; Slocombe, M.; Maher, S.; Vasey, M.; Christian, P.; Lynch, P. Unpiloted aerial system (UAS)-supported biogeomorphic analysis of restored sierra nevada montane meadows. *Remote Sens.* **2020**, *12*, 1828. <https://doi.org/10.3390/rs12111828>.
31. Liang, L.; Qin, Z.; Zhao, S.; Di, L.; Zhang, C.; Deng, M.; Lin, H.; Zhang, L.; Wang, L.; Liu, Z. Estimating crop chlorophyll content with hyperspectral vegetation indices and the hybrid inversion method. *Int. J. Remote Sens.* **2016**, *37*, 2923–2949. <https://doi.org/10.1080/01431161.2016.1186850>.
32. Legleiter, C.J.; Roberts, D.A. A forward image model for passive optical remote sensing of river bathymetry. *Remote Sens. Environ.* **2009**, *113*, 1025–1045. <https://doi.org/10.1016/j.rse.2009.01.018>.
33. Flynn, K.; Chapra, S. Remote Sensing of Submerged Aquatic Vegetation in a Shallow Non-Turbid River Using an Unmanned Aerial Vehicle. *Remote Sens.* **2014**, *6*, 12815–12836. <https://doi.org/10.3390/rs61212815>.
34. Dufour, S.; Rodríguez-González, P.M.; Laslier, M. Tracing the scientific trajectory of riparian vegetation studies: Main topics, approaches and needs in a globally changing world. *Sci. Total Environ.* **2019**, *653*, 1168–1185. <https://doi.org/10.1016/j.scitotenv.2018.10.383>.
35. Poledníková, Z.; Galia, T. Ecosystem Services of Large Wood: Mapping the Research Gap. *Water* **2021**, *13*, 2594. <https://doi.org/10.3390/w13182594>.
36. Feinerer, I.; Hornik, K.; Meyer, D. Text Mining Infrastructure in R. *J. Stat. Softw.* **2008**, *25*, 1–17. <https://doi.org/10.18637/jss.v025.i05>.
37. Rajaraman, A.; Ullman, J.D. Data Mining. In *Mining of Massive Datasets*; Cambridge University Press: Cambridge, UK, 2011; pp. 1–17.
38. Wolman, M.G. A method of sampling coarse river-bed material. *Trans. Am. Geophys. Union* **1954**, *35*, 951–956. <https://doi.org/10.1029/TR035I006P00951>.
39. Dugdale, S.J.; Carbonneau, P.E.; Campbell, D. Aerial photosieving of exposed gravel bars for the rapid calibration of airborne grain size maps. *Earth Surf. Process. Landf.* **2010**, *35*, 627–639. <https://doi.org/10.1002/ESP.1936>.
40. Carbonneau, P.E.; Lane, S.N.; Bergeron, N.E. Catchment-scale mapping of surface grain size in gravel bed rivers using airborne digital imagery. *Water Resour. Res.* **2004**, *40*, W07202. <https://doi.org/10.1029/2003WR002759>.
41. Verdú, J.M.; Batalla, R.J.; Martínez-Casasnovas, J.A. High-resolution grain-size characterisation of gravel bars using imagery analysis and geo-statistics. *Geomorphology* **2005**, *72*, 73–93. <https://doi.org/10.1016/J.GEOMORPH.2005.04.015>.

42. Woodget, A.S.; Austrums, R. Subaerial gravel size measurement using topographic data derived from a UAV-SfM approach. *Earth Surf. Process. Landf.* **2017**, *42*, 1434–1443. <https://doi.org/10.1002/esp.4139>.
43. Woodget, A.S.; Fyffe, C.; Carbonneau, P.E. From manned to unmanned aircraft: Adapting airborne particle size mapping methodologies to the characteristics of sUAS and SfM. *Earth Surf. Process. Landf.* **2018**, *43*, 857–870. <https://doi.org/10.1002/ESP.4285>.
44. Woodget, A.S.; Carbonneau, P.E.; Visser, F.; Maddock, I.P. Quantifying submerged fluvial topography using hyperspatial resolution UAS imagery and structure from motion photogrammetry. *Earth Surf. Process. Landf.* **2015**, *40*, 47–64. <https://doi.org/10.1002/esp.3613>.
45. Dietrich, J.T. Bathymetric Structure-from-Motion: Extracting shallow stream bathymetry from multi-view stereo photogrammetry. *Earth Surf. Process. Landf.* **2017**, *42*, 355–364. <https://doi.org/10.1002/esp.4060>.
46. Pearce, S.; Ljubičić, R.; Peña-Haro, S.; Perks, M.; Tauro, F.; Pizarro, A.; Dal Sasso, S.; Strelnikova, D.; Grimaldi, S.; Maddock, I.; et al. An Evaluation of Image Velocimetry Techniques under Low Flow Conditions and High Seeding Densities Using Unmanned Aerial Systems. *Remote Sens.* **2020**, *12*, 232. <https://doi.org/10.3390/rs12020232>.
47. Marcus, W.A.; Legleiter, C.J.; Aspinall, R.J.; Boardman, J.W.; Crabtree, R.L. High spatial resolution hyperspectral mapping of in-stream habitats, depths, and woody debris in mountain streams. *Geomorphology* **2003**, *55*, 363–380. [https://doi.org/10.1016/S0169-555X\(03\)00150-8](https://doi.org/10.1016/S0169-555X(03)00150-8).
48. Marcus, W.A. Mapping of stream microhabitats with high spatial resolution hyperspectral imagery. *J. Geogr. Syst.* **2002**, *4*, 113–126. <https://doi.org/10.1007/S101090100078>.
49. Lorang, M.S.; Whited, D.C.; Hauer, F.R.; Kimball, J.S.; Stanford, J.A. Using airborne multispectral imagery to evaluate geomorphic work across floodplains of gravel-bed rivers. *Ecol. Appl.* **2005**, *15*, 1209–1222. <https://doi.org/10.1890/03-5290>.
50. Woodget, A.S.; Visser, F.; Maddock, I.P.; Carbonneau, P.E. The Accuracy and Reliability of Traditional Surface Flow Type Mapping: Is it Time for a New Method of Characterizing Physical River Habitat? *River Res. Appl.* **2016**, *32*, 1902–1914. <https://doi.org/10.1002/rra.3047>.
51. Kalacska, M.; Lucanus, O.; Sousa, L.; Vieira, T.; Arroyo-Mora, J. Freshwater Fish Habitat Complexity Mapping Using Above and Underwater Structure-From-Motion Photogrammetry. *Remote Sens.* **2018**, *10*, 1912. <https://doi.org/10.3390/rs10121912>.
52. Casado, M.; Gonzalez, R.; Kriechbaumer, T.; Veal, A. Automated Identification of River Hydromorphological Features Using UAV High Resolution Aerial Imagery. *Sensors* **2015**, *15*, 27969–27989. <https://doi.org/10.3390/s151127969>.
53. Woodget, A.S.; Austrums, R.; Maddock, I.P.; Habit, E. Drones and digital photogrammetry: From classifications to continuums for monitoring river habitat and hydromorphology. *Wiley Interdiscip. Rev. Water* **2017**, *4*, e1222. <https://doi.org/10.1002/wat2.1222>.
54. Konrad, C.P.; Black, R.W.; Voss, F.; Neale, C.M.U. Integrating remotely acquired and field data to assess effects of setback levees on riparian and aquatic habitat in glacial-melt water rivers. *River Res. Appl.* **2008**, *24*, 355–372. <https://doi.org/10.1002/rra.1070>.
55. Hauer, F.R.; Lorang, M.S. River regulation, decline of ecological resources, and potential for restoration in a semi-arid lands river in the western USA. *Aquat. Sci.* **2004**, *66*, 388–401. <https://doi.org/10.1007/s00027-004-0724-7>.
56. Tamminga, A.; Hugenholtz, C.; Eaton, B.; Lapointe, M. Hyperspatial Remote Sensing of Channel Reach Morphology and Hydraulic Fish Habitat Using an Unmanned Aerial Vehicle (UAV): A First Assessment in the Context of River Research and Management. *River Res. Appl.* **2015**, *31*, 379–391. <https://doi.org/10.1002/rra.2743>.
57. Carbonneau, P.E.; Bergeron, N.; Lane, S.N. Automated grain size measurements from airborne remote sensing for long profile measurements of fluvial grain sizes. *Water Resour. Res.* **2005**, *41*, 1–9. <https://doi.org/10.1029/2005WR003994>.
58. Black, M.; Carbonneau, P.; Church, M.; Warburton, J. Mapping sub-pixel fluvial grain sizes with hyperspatial imagery. *Sedimentology* **2014**, *61*, 691–711. <https://doi.org/10.1111/sed.12072>.
59. Lang, N.; Irniger, A.; Rozniak, A.; Hunziker, R.; Wegner, J.D.; Schindler, K. GRAINet: Mapping grain size distributions in river beds from UAV images with convolutional neural networks. *Hydrol. Earth Syst. Sci.* **2021**, *25*, 2567–2597. <https://doi.org/10.5194/hess-25-2567-2021>.
60. Langhammer, J.; Lendziach, T.; Mišijovský, J.; Hartvich, F. UAV-Based Optical Granulometry as Tool for Detecting Changes in Structure of Flood Depositions. *Remote Sens.* **2017**, *9*, 240. <https://doi.org/10.3390/rs9030240>.
61. Carbonneau, P.E.; Bizzi, S.; Marchetti, G. Robotic photosieving from low-cost multirotor sUAS: A proof-of-concept. *Earth Surf. Process. Landf.* **2018**, *43*, 1160–1166. <https://doi.org/10.1002/esp.4298>.
62. Legleiter, C.J.; Overstreet, B.T. Mapping gravel bed river bathymetry from space. *J. Geophys. Res. Earth Surf.* **2012**, *117*, F04024. <https://doi.org/10.1029/2012JF002539>.
63. Legleiter, C.J. Mapping River Depth from Publicly Available Aerial Images. *River Res. Appl.* **2013**, *29*, 760–780. <https://doi.org/10.1002/rra.2560>.
64. Legleiter, C.J. Inferring river bathymetry via Image-to-Depth Quantile Transformation (IDQT). *Water Resour. Res.* **2016**, *52*, 3722–3741. <https://doi.org/10.1002/2016WR018730>.
65. Flener, C. Estimating deep water radiance in shallow water: Adapting optical bathymetry modelling to shallow river environments. *Boreal Environ. Res.* **2013**, *18*, 488–502.
66. Westaway, R.M.; Lane, S.N.; Hicks, D.M. Remote survey of large-scale braided, gravel-bed rivers using digital photogrammetry and image analysis. *Int. J. Remote Sens.* **2003**, *24*, 795–815. <https://doi.org/10.1080/01431160110113070>.

67. Brasington, J.; Langham, J.; Rumsby, B. Methodological sensitivity of morphometric estimates of coarse fluvial sediment transport. *Geomorphology* **2003**, *53*, 299–316. [https://doi.org/10.1016/S0169-555X\(02\)00320-3](https://doi.org/10.1016/S0169-555X(02)00320-3).
68. Williams, R.D.; Brasington, J.; Vericat, D.; Hicks, D.M. Hyperscale terrain modelling of braided rivers: Fusing mobile terrestrial laser scanning and optical bathymetric mapping. *Earth Surf. Process. Landf.* **2014**, *39*, 167–183. <https://doi.org/10.1002/esp.3437>.
69. Javernick, L.; Brasington, J.; Caruso, B. Modeling the topography of shallow braided rivers using Structure-from-Motion photogrammetry. *Geomorphology* **2014**, *213*, 166–182. <https://doi.org/10.1016/j.geomorph.2014.01.006>.
70. Flener, C.; Vaaja, M.; Jaakkola, A.; Krooks, A.; Kaartinen, H.; Kukko, A.; Kasvi, E.; Hyyppä, H.; Hyyppä, J.; Alho, P. Seamless Mapping of River Channels at High Resolution Using Mobile LiDAR and UAV-Photography. *Remote Sens.* **2013**, *5*, 6382–6407. <https://doi.org/10.3390/rs5126382>.
71. Lejot, J.; Delacourt, C.; Piégay, H.; Fournier, T.; Trémélo, M.-L.; Allemand, P. Very high spatial resolution imagery for channel bathymetry and topography from an unmanned mapping controlled platform. *Earth Surf. Process. Landf.* **2007**, *32*, 1705–1725. <https://doi.org/10.1002/esp.1595>.
72. Legleiter, C.J.; Kinzel, P.J. Improving Remotely Sensed River Bathymetry by Image-Averaging. *Water Resour. Res.* **2021**, *57*, e2020WR028795. <https://doi.org/10.1029/2020WR028795>.
73. Legleiter, C.J.; Harrison, L.R. Remote Sensing of River Bathymetry: Evaluating a Range of Sensors, Platforms, and Algorithms on the Upper Sacramento River, California, USA. *Water Resour. Res.* **2019**, *55*, 2142–2169. <https://doi.org/10.1029/2018WR023586>.
74. Legleiter, C.J. Calibrating remotely sensed river bathymetry in the absence of field measurements: Flow Resistance Equation-Based Imaging of River Depths (FREEBIRD). *Water Resour. Res.* **2015**, *51*, 2865–2884. <https://doi.org/10.1002/2014WR016624>.
75. Fonstad, M.A.; Marcus, W.A. Remote sensing of stream depths with hydraulically assisted bathymetry (HAB) models. *Geomorphology* **2005**, *72*, 320–339. <https://doi.org/10.1016/j.geomorph.2005.06.005>.
76. Legleiter, C.J.; Roberts, D.A. Effects of channel morphology and sensor spatial resolution on image-derived depth estimates. *Remote Sens. Environ.* **2005**, *95*, 231–247. <https://doi.org/10.1016/j.rse.2004.12.013>.
77. Legleiter, C.; Fosness, R. Defining the Limits of Spectrally Based Bathymetric Mapping on a Large River. *Remote Sens.* **2019**, *11*, 665. <https://doi.org/10.3390/rs11060665>.
78. Carbonneau, P.E.; Lane, S.N.; Bergeron, N. Feature based image processing methods applied to bathymetric measurements from airborne remote sensing in fluvial environments. *Earth Surf. Process. Landf.* **2006**, *31*, 1413–1423. <https://doi.org/10.1002/esp.1341>.
79. Legleiter, C.; Overstreet, B.; Kinzel, P. Sampling Strategies to Improve Passive Optical Remote Sensing of River Bathymetry. *Remote Sens.* **2018**, *10*, 935. <https://doi.org/10.3390/rs10060935>.
80. Westaway, R.M.; Lane, S.N.; Hicks, D.M. Remote Sensing of Clear-Water, Shallow, Gravel-Bed Rivers Using Digital Photogrammetry. *Photogramm. Eng. Remote Sens.* **2001**, *67*, 1271–1281.
81. Westaway, R.M.; Lane, S.N.; Hicks, D.M. The development of an automated correction procedure for digital photogrammetry for the study of wide, shallow, gravel-bed rivers. *Earth Surf. Process. Landf.* **2000**, *25*, 209–226. [https://doi.org/10.1002/\(SICI\)1096-9837\(200002\)25:2<209::AID-ESP84>3.0.CO;2-Z](https://doi.org/10.1002/(SICI)1096-9837(200002)25:2<209::AID-ESP84>3.0.CO;2-Z).
82. Kasvi, E.; Salmela, J.; Lotsari, E.; Kumpula, T.; Lane, S.N. Comparison of remote sensing based approaches for mapping bathymetry of shallow, clear water rivers. *Geomorphology* **2019**, *333*, 180–197. <https://doi.org/10.1016/j.geomorph.2019.02.017>.
83. Woodget, A.S.; Dietrich, J.T.; Wilson, R.T. Quantifying Below-Water Fluvial Geomorphic Change: The Implications of Refraction Correction, Water Surface Elevations, and Spatially Variable Error. *Remote Sens.* **2019**, *11*, 2415. <https://doi.org/10.3390/rs11202415>.
84. Kinzel, P.; Legleiter, C. sUAS-Based Remote Sensing of River Discharge Using Thermal Particle Image Velocimetry and Bathymetric Lidar. *Remote Sens.* **2019**, *11*, 2317. <https://doi.org/10.3390/rs11192317>.
85. Eltner, A.; Bertalan, L.; Grundmann, J.; Perks, M.T.; Lotsari, E. Hydro-morphological mapping of river reaches using videos captured with UAS. *Earth Surf. Process. Landforms* **2021**, *46*, 2773–2787. <https://doi.org/10.1002/esp.5205>.
86. Eltner, A.; Sardemann, H.; Grundmann, J. Technical Note: Flow velocity and discharge measurement in rivers using terrestrial and unmanned-aerial-vehicle imagery. *Hydrol. Earth Syst. Sci.* **2020**, *24*, 1429–1445. <https://doi.org/10.5194/hess-24-1429-2020>.
87. Strelnikova, D.; Paulus, G.; Käfer, S.; Anders, K.-H.; Mayr, P.; Mader, H.; Scherling, U.; Schneeberger, R. Drone-Based Optical Measurements of Heterogeneous Surface Velocity Fields around Fish Passages at Hydropower Dams. *Remote Sens.* **2020**, *12*, 384. <https://doi.org/10.3390/rs12030384>.
88. Tauro, F.; Porfiri, M.; Grimaldi, S. Surface flow measurements from drones. *J. Hydrol.* **2016**, *540*, 240–245. <https://doi.org/10.1016/j.jhydrol.2016.06.012>.
89. Perks, M.T.; Dal Sasso, S.F.; Hauet, A.; Jamieson, E.; Le Coz, J.; Pearce, S.; Peña-Haro, S.; Pizarro, A.; Strelnikova, D.; Tauro, F.; et al. Towards harmonisation of image velocimetry techniques for river surface velocity observations. *Earth Syst. Sci. Data* **2020**, *12*, 1545–1559. <https://doi.org/10.5194/essd-12-1545-2020>.
90. Pizarro, A.; Dal Sasso, S.F.; Manfreda, S. Refining image-velocimetry performances for streamflow monitoring: Seeding metrics to errors minimization. *Hydrol. Process.* **2020**, *34*, 5167–5175. <https://doi.org/10.1002/hyp.13919>.
91. Kuhn, J.; Casas-Mulet, R.; Pander, J.; Geist, J. Assessing stream thermal heterogeneity and cold-water patches from UAV-based imagery: A matter of classification methods and metrics. *Remote Sens.* **2021**, *13*, 1379. <https://doi.org/10.3390/rs13071379>.

92. Dugdale, S.J.; Kelleher, C.A.; Malcolm, I.A.; Caldwell, S.; Hannah, D.M. Assessing the potential of drone-based thermal infrared imagery for quantifying river temperature heterogeneity. *Hydrol. Process.* **2019**, *33*, 1152–1163. <https://doi.org/10.1002/hyp.13395>.
93. Tonolla, D.; Wolter, C.; Ruhtz, T.; Tockner, K. Linking fish assemblages and spatiotemporal thermal heterogeneity in a river-floodplain landscape using high-resolution airborne thermal infrared remote sensing and in-situ measurements. *Remote Sens. Environ.* **2012**, *125*, 134–146. <https://doi.org/10.1016/j.rse.2012.07.014>.
94. Dugdale, S.J.; Hannah, D.M.; Malcolm, I.A. An evaluation of different forest cover geospatial data for riparian shading and river temperature modelling. *River Res. Appl.* **2020**, *36*, 709–723. <https://doi.org/10.1002/rra.3598>.
95. Dugdale, S.J.; Malcolm, I.A.; Hannah, D.M. Drone-based Structure-from-Motion provides accurate forest canopy data to assess shading effects in river temperature models. *Sci. Total Environ.* **2019**, *678*, 326–340. <https://doi.org/10.1016/j.scitotenv.2019.04.229>.
96. Willis, A.; Holmes, E. Eye in the Sky: Using UAV imagery of seasonal riverine canopy growth to model water temperature. *Hydrology* **2019**, *6*, 6. <https://doi.org/10.3390/hydrology6010006>.
97. Seixas, G.B.; Beechie, T.J.; Fogel, C.; Kiffney, P.M. Historical and Future Stream Temperature Change Predicted by a Lidar-Based Assessment of Riparian Condition and Channel Width. *J. Am. Water Resour. Assoc.* **2018**, *54*, 974–991. <https://doi.org/10.1111/1752-1688.12655>.
98. Kałuża, T.; Sojka, M.; Wróżyński, R.; Jaskuła, J.; Zaborowski, S.; Hämmerling, M. Modeling of river channel shading as a factor for changes in hydromorphological conditions of small lowland rivers. *Water* **2020**, *12*, 527. <https://doi.org/10.3390/w12020527>.
99. Loicq, P.; Moatar, F.; Jullian, Y.; Dugdale, S.J.; Hannah, D.M. Improving representation of riparian vegetation shading in a regional stream temperature model using LiDAR data. *Sci. Total Environ.* **2018**, *624*, 480–490. <https://doi.org/10.1016/j.scitotenv.2017.12.129>.
100. Greenberg, J.A.; Hestir, E.L.; Riano, D.; Scheer, G.J.; Ustin, S.L. Using LiDAR Data Analysis to Estimate Changes in Insolation Under Large-Scale Riparian Deforestation. *J. Am. Water Resour. Assoc.* **2012**, *48*, 939–948. <https://doi.org/10.1111/j.1752-1688.2012.00664.x>.
101. Johansen, K.; Grove, J.; Denham, R.; Phinn, S. Assessing stream bank condition using airborne LiDAR and high spatial resolution image data in temperate semirural areas in Victoria, Australia. *J. Appl. Remote Sens.* **2013**, *7*, 073492. <https://doi.org/10.1117/1.jrs.7.073492>.
102. Timm, R.K.; Caldwell, L.; Nelson, A.; Long, C.; Chilibeck, M.B.; Johnson, M.; Ross, K.; Muller, A.; Brown, J.M. Drones, hydraulics, and climate change: Inferring barriers to steelhead spawning migrations. *WIREs Water* **2019**, *6*, e1379. <https://doi.org/10.1002/wat2.1379>.
103. Entwistle, N.; Heritage, G.; Milan, D. Ecohydraulic modelling of anabranching rivers. *River Res. Appl.* **2019**, *35*, 353–364. <https://doi.org/10.1002/rra.3413>.
104. Wyrick, J.R.; Pasternack, G.B. Geospatial organization of fluvial landforms in a gravel–cobble river: Beyond the riffle–pool couplet. *Geomorphology* **2014**, *213*, 48–65. <https://doi.org/10.1016/j.geomorph.2013.12.040>.
105. Hauer, C.; Mandlbürger, G.; Schober, B.; Habersack, H. Morphologically related integrative management concept for reconnecting abandoned channels based on airborne lidar data and habitat modelling. *River Res. Appl.* **2014**, *30*, 537–556. <https://doi.org/10.1002/rra.2593>.
106. Hajdukiewicz, M.; Wyzga, B.; Hajdukiewicz, H.; Mikuś, P. Photogrammetric reconstruction of changes in vertical river position using archival aerial photos: Case study of the Czarny Dunajec River, Polish Carpathians. *Acta Geophys.* **2019**, *67*, 1–17. <https://doi.org/10.1007/s11600-019-00307-0>.
107. Poole, G.C.; Stanford, J.A.; Frissell, C.A.; Running, S.W. Three-dimensional mapping of geomorphic controls on flood-plain hydrology and connectivity from aerial photos. *Geomorphology* **2002**, *48*, 329–347. [https://doi.org/10.1016/S0169-555X\(02\)00078-8](https://doi.org/10.1016/S0169-555X(02)00078-8).
108. Hicks, D.M.; Shankar, U.; Duncan, M.J.; Rebuff, M.; Aberle, J. Use of Remote-Sensing with Two-Dimensional Hydrodynamic Models to Assess Impacts of Hydro-Operations on a Large, Braided, Gravel-Bed River: Waitaki River, New Zealand. In *Braided Rivers*; Blackwell Publishing Ltd.: Oxford, UK, 2009; pp. 311–326.
109. Nuhličková, S.; Svetlík, J.; Šibíková, M.; Jarolímek, I.; Zuna-Kratky, T. Current distribution, microhabitat requirements and vulnerability of the Keeled Plump Bush-cricket (*Isophya costata*) at the north-western periphery of its range. *J. Insect Conserv.* **2021**, *25*, 65–76. <https://doi.org/10.1007/s10841-020-00280-w>.
110. Ulloa, H.; Iroumé, A.; Mao, L.; Andreoli, A.; Diez, S.; Lara, L.E. Use of Remote Imagery to Analyse Changes in Morphology and Longitudinal Large Wood Distribution in the Blanco River After the 2008 Chaitén Volcanic Eruption, Southern Chile. *Geogr. Ann. Ser. A Phys. Geogr.* **2015**, *97*, 523–541. <https://doi.org/10.1111/geoa.12091>.
111. MacVicar, B.J.; Piégay, H.; Henderson, A.; Comiti, F.; Oberlin, C.; Pecorari, E. Quantifying the temporal dynamics of wood in large rivers: Field trials of wood surveying, dating, tracking, and monitoring techniques. *Earth Surf. Process. Landf.* **2009**, *34*, 2031–2046. <https://doi.org/10.1002/ESP.1888>.
112. Gurnell, A.M.; Bickerton, M.; Angold, P.; Bell, D.; Morrissey, I.; Petts, G.E.; Sadler, J. Morphological and ecological change on a meander bend: The role of hydrological processes and the application of GIS. *Hydrol. Processes* **1998**, *12*, 981–993.
113. Gilvear, D.; Willby, N. Channel dynamics and geomorphic variability as controls on gravel bar vegetation; River Tummel, Scotland. *River Res. Appl.* **2006**, *22*, 457–474. <https://doi.org/10.1002/rra.917>.

114. Angiolini, C.; Nucci, A.; Frignani, F.; Landi, M. Using multivariate analyses to assess effects of fluvial type on plant species distribution in a Mediterranean river. *Wetlands* **2011**, *31*, 167–177. <https://doi.org/10.1007/s13157-010-0118-7>.
115. Tiegs, S.D.; O’leary, J.F.; Pohl, M.M.; Munill, C.L. Flood disturbance and riparian species diversity on the Colorado River Delta. *Biodivers. Conserv.* **2005**, *14*, 1175–1194. <https://doi.org/10.1007/s10531-004-7841-4>.
116. Choi, S.U.; Yoon, B.; Woo, H. Effects of dam-induced flow regime change on downstream river morphology and vegetation cover in the Hwang River, Korea. *River Res. Appl.* **2005**, *21*, 315–325. <https://doi.org/10.1002/rra.849>.
117. Birken, A.S.; Cooper, D.J. Processes of tamarix invasion and floodplain development along the lower green river, Utah. *Ecol. Appl.* **2006**, *16*, 1103–1120.
118. Townsend, P.A. Relationships between vegetation patterns and hydroperiod on the Roanoke River floodplain, North Carolina. *Plant Ecol.* **2001**, *156*, 43–58.
119. Polzin, M.L.; Rood, S.B. Effective disturbance: Seedling safe sites and patch recruitment of riparian cottonwoods after a major flood of a mountain river. *WETLANDS* **2006**, *26*, 965–980. [https://doi.org/10.1672/0277-5212\(2006\)26\[965:EDSSSA\]2.0.CO;2](https://doi.org/10.1672/0277-5212(2006)26[965:EDSSSA]2.0.CO;2).
120. Cienciala, P.; Nelson, A.D.; Haas, A.D.; Xu, Z. Lateral geomorphic connectivity in a fluvial landscape system: Unraveling the role of confinement, biogeomorphic interactions, and glacial legacies. *Geomorphology* **2020**, *354*, 107036. <https://doi.org/10.1016/j.geomorph.2020.107036>.
121. Yousefi, S.; Pourghasemi, H.R.; Hooke, J.; Navratil, O.; Kidová, A. Changes in morphometric meander parameters identified on the Karoon River, Iran, using remote sensing data. *Geomorphology* **2016**, *271*, 55–64. <https://doi.org/10.1016/j.geomorph.2016.07.034>.
122. Bhunia, G.S.; Shit, P.K.; Pal, D.K. Channel dynamics associated with land use/cover change in Ganges river, India, 1989–2010. *Spat. Inf. Res.* **2016**, *24*, 437–449. <https://doi.org/10.1007/s41324-016-0045-7>.
123. Yousefi, S.; Moradi, H.R.; Pourghasemi, H.R.; Khatami, R. Assessment of floodplain landuse and channel morphology within meandering reach of the Talar River in Iran using GIS and aerial photographs. *Geocarto Int.* **2018**, *33*, 1367–1380. <https://doi.org/10.1080/10106049.2017.1353645>.
124. Michalková, M.; Piégay, H.; Kondolf, G.M.; Greco, S.E. Lateral erosion of the Sacramento River, California (1942–1999), and responses of channel and floodplain lake to human influences. *Earth Surf. Process. Landf.* **2011**, *36*, 257–272. <https://doi.org/10.1002/esp.2106>.
125. Segura-Beltrán, F.; Sanchis-Ibor, C. Assessment of channel changes in a Mediterranean ephemeral stream since the early twentieth century. The Rambla de Cervera, eastern Spain. *Geomorphology* **2013**, *201*, 199–214. <https://doi.org/10.1016/j.geomorph.2013.06.021>.
126. Llena, M.; Vericat, D.; Martínez-Casasnovas, J.A.; Smith, M.W. Geomorphic adjustments to multi-scale disturbances in a mountain river: A century of observations. *CATENA* **2020**, *192*, 104584. <https://doi.org/10.1016/j.catena.2020.104584>.
127. Surian, N.; Ziliani, L.; Comiti, F.; Lenzi, M.A.; Mao, L. Channel adjustments and alteration of sediment fluxes in gravel-bed rivers of North-Eastern Italy: Potentials and limitations for channel recovery. *River Res. Appl.* **2009**, *25*, 551–567. <https://doi.org/10.1002/rra.1231>.
128. Greco, S.E.; Fremier, A.K.; Larsen, E.W.; Plant, R.E. A tool for tracking floodplain age land surface patterns on a large meandering river with applications for ecological planning and restoration design. *Landsc. Urban Plan.* **2007**, *81*, 354–373. <https://doi.org/10.1016/J.LANDURBPLAN.2007.01.002>.
129. Rusnák, M.; Sládek, J.; Pacina, J.; Kidová, A. Monitoring of avulsion channel evolution and river morphology changes using UAV photogrammetry: Case study of the gravel bed Ondava River in Outer Western Carpathians. *Area* **2019**, *51*, 549–560. <https://doi.org/10.1111/area.12508>.
130. Surian, N.; Barban, M.; Ziliani, L.; Monegato, G.; Bertoldi, W.; Comiti, F. Vegetation turnover in a braided river: Frequency and effectiveness of floods of different magnitude. *Earth Surf. Process. Landf.* **2015**, *40*, 542–558. <https://doi.org/10.1002/esp.3660>.
131. Philipsen, L.J.; Romuld, M.A.; Rood, S.B. Floodplain forest dynamics: Half-century floods enable pulses of geomorphic disturbance and cottonwood colonization along a prairie river. *River Res. Appl.* **2021**, *37*, 64–77. <https://doi.org/10.1002/rra.3740>.
132. Sanchis-Ibor, C.; Segura-Beltrán, F.; Navarro-Gómez, A. Channel forms and vegetation adjustment to damming in a Mediterranean gravel-bed river (Serpis River, Spain). *River Res. Appl.* **2019**, *35*, 37–47. <https://doi.org/10.1002/rra.3381>.
133. Casado, A.; Peiry, J.L.; Campo, A.M. Geomorphic and vegetation changes in a meandering dryland river regulated by a large dam, Sauce Grande River, Argentina. *Geomorphology* **2016**, *268*, 21–34. <https://doi.org/10.1016/j.geomorph.2016.05.036>.
134. Magdaleno, F.; Fernández, J.A. Hydromorphological alteration of a large Mediterranean river: Relative role of high and low flows on the evolution of riparian forests and channel morphology. *River Res. Appl.* **2011**, *27*, 374–387. <https://doi.org/10.1002/rra.1368>.
135. Marteau, B.; Vericat, D.; Gibbins, C.; Batalla, R.J.; Green, D.R. Application of Structure-from-Motion photogrammetry to river restoration. *Earth Surf. Process. Landf.* **2017**, *42*, 503–515. <https://doi.org/10.1002/esp.4086>.
136. Forzieri, G.; Degetto, M.; Righetti, M.; Castelli, F.; Preti, F. Satellite multispectral data for improved floodplain roughness modelling. *J. Hydrol.* **2011**, *407*, 41–57. <https://doi.org/10.1016/j.jhydrol.2011.07.009>.
137. Choné, G.; Biron, P.M. Assessing the Relationship between River Mobility and Habitat. *River Res. Appl.* **2016**, *32*, 528–539. <https://doi.org/10.1002/rra.2896>.

138. Frazier, P.; Ryder, D.; McIntyre, E.; Stewart, M. Understanding riverine habitat inundation patterns: Remote sensing tools and techniques. *Wetlands* **2012**, *32*, 225–237. <https://doi.org/10.1007/s13157-011-0229-9>.
139. White, M.S.; Tavernia, B.G.; Shafroth, P.B.; Chapman, T.B.; Sanderson, J.S. Vegetative and geomorphic complexity at tributary junctions on the Colorado and Dolores Rivers: A blueprint for riparian restoration. *Landsc. Ecol.* **2018**, *33*, 2205–2220. <https://doi.org/10.1007/s10980-018-0734-9>.
140. Doering, M.; Blaurock, M.; Robinson, C.T. Landscape transformation of an Alpine floodplain influenced by humans: Historical analyses from aerial images. *Hydrol. Process.* **2012**, *26*, 3319–3326. <https://doi.org/10.1002/hyp.8374>.
141. Hohensinner, S.; Jungwirth, M.; Muhar, S.; Schmutz, S. Spatio-temporal habitat dynamics in a changing Danube River landscape 1812–2006. *River Res. Appl.* **2011**, *27*, 939–955. <https://doi.org/10.1002/rra.1407>.
142. MacNally, R.; Parkinson, A.; Horrocks, G.; Young, M. Current loads of coarse woody debris on southeastern Australian floodplains: Evaluation of change and implications for restoration. *Restor. Ecol.* **2002**, *10*, 627–635. <https://doi.org/10.1046/j.1526-100X.2002.01043.x>.
143. Rusnák, M.; Sládek, J.; Kidová, A.; Lehotský, M. Template for high-resolution river landscape mapping using UAV technology. *Measurement* **2018**, *115*, 139–151. <https://doi.org/10.1016/j.measurement.2017.10.023>.
144. Shields, F.D. Woody vegetation and riprap stability along the sacramento river mile 84.5–119. *J. Am. Water Resour. Assoc.* **1991**, *27*, 527–536. <https://doi.org/10.1111/j.1752-1688.1991.tb01453.x>.
145. Cline, S.P.; McAllister, L.S. Plant succession after hydrologic disturbance: Inferences from contemporary vegetation on a chronosequence of bars, Willamette River, Oregon, USA. *River Res. Appl.* **2012**, *28*, 1519–1539. <https://doi.org/10.1002/rra.1539>.
146. Ikeda, H.; Iimura, K.; Komura, S.; Kawashima, C.; Sato, W. Vegetation transition and coarse sediment movement after gravel bar restoration with two meandering lanes in a steep river. *J. Hydro-Environ. Res.* **2020**, *30*, 25–34. <https://doi.org/10.1016/j.jher.2019.11.004>.
147. Kamisako, M.; Sannoh, K.; Kamitani, T. Does understory vegetation reflect the history of fluvial disturbance in a riparian forest? *Ecol. Res.* **2007**, *22*, 67–74. <https://doi.org/10.1007/s11284-006-0002-3>.
148. Hazarika, N.; Das, A.K.; Borah, S.B. Assessing land-use changes driven by river dynamics in chronically flood affected Upper Brahmaputra plains, India, using RS-GIS techniques. *Egypt. J. Remote Sens. Sp. Sci.* **2015**, *18*, 107–118. <https://doi.org/10.1016/j.ejrs.2015.02.001>.
149. Kondolf, G.M.; Piégay, H.; Landon, N. Changes in the riparian zone of the lower Eygues River, France, since 1830. *Landsc. Ecol.* **2007**, *22*, 367–384. <https://doi.org/10.1007/s10980-006-9033-y>.
150. Bertalan, L.; Novák, T.; Németh, Z.; Rodrigo-Comino, J.; Kertész, Á.; Szabó, S. Issues of Meander Development: Land Degradation or Ecological Value? The Example of the Sajó River, Hungary. *Water* **2018**, *10*, 1613. <https://doi.org/10.3390/w10111613>.
151. García de Jalón, D.; Martínez-Fernández, V.; Fazelpoor, K.; González del Tánago, M. Vegetation encroachment ratios in regulated and non-regulated Mediterranean rivers (Spain): An exploratory overview. *J. Hydro-Environ. Res.* **2020**, *30*, 35–44. <https://doi.org/10.1016/j.jher.2019.11.006>.
152. Magdaleno, F.; Anastasio Fernández, J.; Merino, S. The Ebro River in the 20th century or the ecomorphological transformation of a large and dynamic Mediterranean channel. *Earth Surf. Process. Landf.* **2012**, *37*, 486–498. <https://doi.org/10.1002/esp.2258>.
153. Cadol, D.; Rathburn, S.L.; Cooper, D.J. Aerial photographic analysis of channel narrowing and vegetation expansion in Canyon De Chelly National Monument, Arizona, USA, 1935–2004. *River Res. Appl.* **2011**, *27*, 841–856. <https://doi.org/10.1002/rra.1399>.
154. Reid, H.E.; Brierley, G.J. Assessing geomorphic sensitivity in relation to river capacity for adjustment. *Geomorphology* **2015**, *251*, 108–121. <https://doi.org/10.1016/j.geomorph.2015.09.009>.
155. Kleinhans, M.; Douma, H.; Addink, E.A. Fate of pioneering vegetation patches in a dynamic meandering river. *Earth Surf. Process. Landf.* **2019**, *44*, 1618–1632. <https://doi.org/10.1002/esp.4596>.
156. Corenblit, D.; Steiger, J.; González, E.; Gurnell, A.M.; Charrier, G.; Darrozes, J.; Dousseau, J.; Julien, F.; Lambs, L.; Larrue, S.; et al. The biogeomorphological life cycle of poplars during the fluvial biogeomorphological succession: A special focus on *Populus nigra* L. *Earth Surf. Process. Landf.* **2014**, *39*, 546–563. <https://doi.org/10.1002/esp.3515>.
157. Corenblit, D.; Tabacchi, E.; Steiger, J.; Gurnell, A.M. Reciprocal interactions and adjustments between fluvial landforms and vegetation dynamics in river corridors: A review of complementary approaches. *Earth-Sci. Rev.* **2007**, *84*, 56–86. <https://doi.org/10.1016/j.earscirev.2007.05.004>.
158. Bertoldi, W.; Gurnell, A.M.; Welber, M. Wood recruitment and retention: The fate of eroded trees on a braided river explored using a combination of field and remotely-sensed data sources. *Geomorphology* **2013**, *180–181*, 146–155. <https://doi.org/10.1016/J.GEOMORPH.2012.10.003>.
159. Bertoldi, W.; Gurnell, A.; Surian, N.; Tockner, K.; Zanoni, L.; Ziliani, L.; Zolezzi, G. Understanding reference processes: Linkages between river flows, sediment dynamics and vegetated landforms along the Tagliamento River, Italy. *River Res. Appl.* **2009**, *25*, 501–516. <https://doi.org/10.1002/rra.1233>.
160. Bertoldi, W.; Gurnell, A.M.; Drake, N.A. The topographic signature of vegetation development along a braided river: Results of a combined analysis of airborne lidar, color air photographs, and ground measurements. *Water Resour. Res.* **2011**, *47*, W06525. <https://doi.org/10.1029/2010WR010319>.

161. Gurnell, A.M.; Bertoldi, W. Extending the conceptual model of river island development to incorporate different tree species and environmental conditions. *River Res. Appl.* **2020**, *36*, 1730–1747. <https://doi.org/10.1002/rra.3691>.
162. Picco, L.; Mao, L.; Rainato, R.; Lenzi, M.A. Medium-term fluvial island evolution in a disturbed gravel-bed river (piave river, northeastern Italian Alps). *Geogr. Ann. Ser. A, Phys. Geogr.* **2014**, *96*, 83–97. <https://doi.org/10.1111/geoa.12034>.
163. Bertoldi, W.; Gurnell, A.M. Physical engineering of an island-braided river by two riparian tree species: Evidence from aerial images and airborne lidar. *River Res. Appl.* **2020**, *36*, rra.3657. <https://doi.org/10.1002/rra.3657>.
164. Corenblit, D.; Steiger, J.; Charrier, G.; Darrozes, J.; Garófano-Gómez, V.; Garreau, A.; González, E.; Gurnell, A.M.; Hortobágyi, B.; Julien, F.; et al. *Populus nigra* L. establishment and fluvial landform construction: Biogeomorphic dynamics within a channelized river. *Earth Surf. Process. Landf.* **2016**, *41*, 1276–1292. <https://doi.org/10.1002/esp.3954>.
165. van Iersel, W.; Straatsma, M.; Addink, E.; Middelkoop, H. Monitoring height and greenness of non-woody floodplain vegetation with UAV time series. *ISPRS J. Photogramm. Remote Sens.* **2018**, *141*, 112–123. <https://doi.org/10.1016/j.isprsjprs.2018.04.011>.
166. Farid, A.; Goodrich, D.C.; Sorooshian, S. Using Airborne Lidar to Discern Age Classes of Cottonwood Trees in a Riparian Area. *West. J. Appl. For.* **2006**, *21*, 149–158. <https://doi.org/10.1093/wjaf/21.3.149>.
167. Johansen, K.; Arroyo, L.A.; Armston, J.; Phinn, S.; Witte, C. Mapping riparian condition indicators in a sub-tropical savanna environment from discrete return LiDAR data using object-based image analysis. *Ecol. Indic.* **2010**, *10*, 796–807. <https://doi.org/10.1016/j.ecolind.2010.01.001>.
168. Picco, L.; Tonon, A.; Ravazzolo, D.; Rainato, R.; Lenzi, M.A. Monitoring river island dynamics using aerial photographs and lidar data: The tagliamento river study case. *Appl. Geomat.* **2015**, *7*, 163–170. <https://doi.org/10.1007/s12518-014-0139-7>.
169. Woellner, R.; Wagner, T.C. Saving species, time and money: Application of unmanned aerial vehicles (UAVs) for monitoring of an endangered alpine river specialist in a small nature reserve. *Biol. Conserv.* **2019**, *233*, 162–175. <https://doi.org/10.1016/j.biocon.2019.02.037>.
170. Hortobágyi, B.; Corenblit, D.; Vautier, F.; Steiger, J.; Roussel, E.; Burkart, A.; Peiry, J.L. A multi-scale approach of fluvial biogeomorphic dynamics using photogrammetry. *J. Environ. Manage.* **2017**, *202*, 348–362. <https://doi.org/10.1016/j.jenvman.2016.08.069>.
171. Abu-Aly, T.R.; Pasternack, G.B.; Wyrick, J.R.; Barker, R.; Massa, D.; Johnson, T. Effects of LiDAR-derived, spatially distributed vegetation roughness on two-dimensional hydraulics in a gravel-cobble river at flows of 0.2 to 20 times bankfull. *Geomorphology* **2014**, *206*, 468–482. <https://doi.org/10.1016/j.geomorph.2013.10.017>.
172. Hoyle, J.; Brooks, A.; Spencer, J. Modelling reach-scale variability in sediment mobility: An approach for within-reach prioritization of river rehabilitation works. *River Res. Appl.* **2012**, *28*, 609–629. <https://doi.org/10.1002/rra.1472>.
173. Forzieri, G.; Guarnieri, L.; Vivoni, E.R.; Castelli, F.; Preti, F. Spectral-ALS data fusion for different roughness parameterizations of forested floodplains. *River Res. Appl.* **2011**, *27*, 826–840. <https://doi.org/10.1002/RRA.1398>.
174. Gurnell, A.M.; Bertoldi, W.; Francis, R.A.; Gurnell, J.; Mardhiah, U. Understanding processes of island development on an island braided river over timescales from days to decades. *Earth Surf. Process. Landforms* **2018**, *44*, 624–640. <https://doi.org/10.1002/esp.4494>.
175. Harms, T.K.; Wentz, E.A.; Grimm, N.B. Spatial heterogeneity of denitrification in semi-arid floodplains. *Ecosystems* **2009**, *12*, 129–143. <https://doi.org/10.1007/s10021-008-9212-6>.
176. Young, J.; Welsch, D.; Deacon, S. Assessing the hydrologic impact of historical railroad embankments on wetland vegetation response in Canaan Valley, West Virginia: The value of high-resolution data. *Restor. Ecol.* **2020**, *28*, 51–62. <https://doi.org/10.1111/rec.13061>.
177. Johansen, K.; Phinn, S.; Witte, C. Mapping of riparian zone attributes using discrete return LiDAR, QuickBird and SPOT-5 imagery: Assessing accuracy and costs. *Remote Sens. Environ.* **2010**, *114*, 2679–2691. <https://doi.org/10.1016/j.rse.2010.06.004>.
178. Straatsma, M.W.; Baptist, M.J. Floodplain roughness parameterization using airborne laser scanning and spectral remote sensing. *Remote Sens. Environ.* **2008**, *112*, 1062–1080. <https://doi.org/10.1016/j.rse.2007.07.012>.
179. McMahon, J.M.; Olley, J.M.; Brooks, A.P.; Smart, J.C.R.; Stewart-Koster, B.; Venables, W.N.; Curwen, G.; Kemp, J.; Stewart, M.; Saxton, N.; et al. Vegetation and longitudinal coarse sediment connectivity affect the ability of ecosystem restoration to reduce riverbank erosion and turbidity in drinking water. *Sci. Total Environ.* **2020**, *707*, 135904. <https://doi.org/10.1016/j.scitotenv.2019.135904>.
180. Laslier, M.; Hubert-Moy, L.; Corpetti, T.; Dufour, S. Monitoring the colonization of alluvial deposits using multitemporal UAV RGB-imagery. *Appl. Veg. Sci.* **2019**, *22*, 561–572. <https://doi.org/10.1111/avsc.12455>.
181. Lan, D.; Rui-Hong, Y. New grassland riparian zone delineation method for calculating ecological water demand to guide management goals. *River Res. Appl.* **2020**, *36*, 1838–1851. <https://doi.org/10.1002/rra.3707>.
182. Henshaw, A.J.; Gurnell, A.M.; Bertoldi, W.; Drake, N.A. An assessment of the degree to which Landsat TM data can support the assessment of fluvial dynamics, as revealed by changes in vegetation extent and channel position, along a large river. *Geomorphology* **2013**, *202*, 74–85. <https://doi.org/10.1016/j.geomorph.2013.01.011>.
183. Park, E.; Latrubesse, E.M. The hydro-geomorphologic complexity of the lower Amazon River floodplain and hydrological connectivity assessed by remote sensing and field control. *Remote Sens. Environ.* **2017**, *198*, 321–332. <https://doi.org/10.1016/j.rse.2017.06.021>.

184. Jia, M.; Mao, D.; Wang, Z.; Ren, C.; Zhu, Q.; Li, X.; Zhang, Y. Tracking long-term floodplain wetland changes: A case study in the China side of the Amur River Basin. *Int. J. Appl. Earth Obs. Geoinf.* **2020**, *92*, 102185. <https://doi.org/10.1016/j.jag.2020.102185>.
185. Rabanaque, M.P.; Martínez-Fernández, V.; Calle, M.; Benito, G. Basin-wide hydromorphological analysis of ephemeral streams using machine learning algorithms ‡. *Earth Surf. Process. Landf.* **2022**, *47*, 328–344. <https://doi.org/10.1002/esp.5250>.
186. Daryaei, A.; Sohrabi, H.; Atzberger, C.; Immitzer, M. Fine-scale detection of vegetation in semi-arid mountainous areas with focus on riparian landscapes using Sentinel-2 and UAV data. *Comput. Electron. Agric.* **2020**, *177*, 105686. <https://doi.org/10.1016/j.compag.2020.105686>.
187. Johansen, K.; Coops, N.C.; Gergel, S.E.; Stange, Y. Application of high spatial resolution satellite imagery for riparian and forest ecosystem classification. *Remote Sens. Environ.* **2007**, *110*, 29–44. <https://doi.org/10.1016/j.rse.2007.02.014>.
188. Morgan, B.E.; Chipman, J.W.; Bolger, D.T.; Dietrich, J.T. Spatiotemporal analysis of vegetation cover change in a large ephemeral river: Multi-sensor fusion of unmanned aerial vehicle (uav) and landsat imagery. *Remote Sens.* **2021**, *13*, 1–24. <https://doi.org/10.3390/rs13010051>.
189. Arroyo, L.A.; Johansen, K.; Armston, J.; Phinn, S. Integration of LiDAR and QuickBird imagery for mapping riparian biophysical parameters and land cover types in Australian tropical savannas. *For. Ecol. Manage.* **2010**, *259*, 598–606. <https://doi.org/10.1016/j.foreco.2009.11.018>.
190. Johansen, K.; Phinn, S. Mapping Structural Parameters and Species Composition of Riparian Vegetation Using IKONOS and Landsat ETM+ Data in Australian Tropical Savannas. *Photogramm. Eng. Remote Sens.* **2006**, *72*, 71–80. <https://doi.org/10.14358/PERS.72.1.71>.
191. Cunningham, S.C.; Mac Nally, R.; Read, J.; Baker, P.J.; White, M.; Thomson, J.R.; Griffioen, P. A robust technique for mapping vegetation condition across a major river system. *Ecosystems* **2009**, *12*, 207–219. <https://doi.org/10.1007/s10021-008-9218-0>.
192. Bertoldi, W.; Drake, N.A.; Gurnell, A.M. Interactions between river flows and colonizing vegetation on a braided river: Exploring spatial and temporal dynamics in riparian vegetation cover using satellite data. *Earth Surf. Process. Landf.* **2011**, *36*, 1474–1486. <https://doi.org/10.1002/esp.2166>.
193. Han, M.; Brierley, G.; Li, B.; Li, Z.; Li, X. Impacts of flow regulation on geomorphic adjustment and riparian vegetation succession along an anabranching reach of the Upper Yellow River. *CATENA* **2020**, *190*, 104561. <https://doi.org/10.1016/J.CATENA.2020.104561>.
194. Ablat, X.; Liu, G.; Liu, Q.; Huang, C. Application of Landsat derived indices and hydrological alteration matrices to quantify the response of floodplain wetlands to river hydrology in arid regions based on different dam operation strategies. *Sci. Total Environ.* **2019**, *688*, 1389–1404. <https://doi.org/10.1016/j.scitotenv.2019.06.232>.
195. Deng, F.; Wang, X.; Cai, X.; Li, E.; Jiang, L.; Li, H.; Yan, R. Analysis of the relationship between inundation frequency and wetland vegetation in Dongting Lake using remote sensing data. *Ecohydrology* **2014**, *7*, 717–726. <https://doi.org/10.1002/ECO.1393>.
196. Hopkinson, C.; Fuoco, B.; Grant, T.; Bayley, S.E.; Brisco, B.; Macdonald, R. Wetland hydroperiod change along the upper columbia river floodplain, canada, 1984 to 2019. *Remote Sens.* **2020**, *12*, 1–20. <https://doi.org/10.3390/rs12244084>.
197. Broich, M.; Tulbure, M.G.; Verbesselt, J.; Xin, Q.; Wearne, J. Quantifying Australia’s dryland vegetation response to flooding and drought at sub-continental scale. *Remote Sens. Environ.* **2018**, *212*, 60–78. <https://doi.org/10.1016/j.rse.2018.04.032>.
198. Chen, L.; Wu, Y.; Xu, Y.J.; Zhang, G. Alteration of flood pulses by damming the Nenjiang River, China—Implication for the need to identify a hydrograph-based inundation threshold for protecting floodplain wetlands. *Ecol. Indic.* **2021**, *124*, 107406. <https://doi.org/10.1016/j.ecolind.2021.107406>.
199. Marchetti, Z.Y.; Ramonell, C.G.; Brumnich, F.; Alberdi, R.; Kandus, P. Vegetation and hydrogeomorphic features of a large lowland river: NDVI patterns summarizing fluvial dynamics and supporting interpretations of ecological patterns. *Earth Surf. Process. Landf.* **2020**, *45*, 694–706. <https://doi.org/10.1002/esp.4766>.
200. Saha, D.; Das, D.; Dasgupta, R.; Patel, P.P. Application of ecological and aesthetic parameters for riparian quality assessment of a small tropical river in eastern India. *Ecol. Indic.* **2020**, *117*, 106627. <https://doi.org/10.1016/j.ecolind.2020.106627>.
201. Langat, P.K.; Kumar, L.; Koech, R.; Ghosh, M.K. Characterisation of channel morphological pattern changes and flood corridor dynamics of the tropical Tana River fluvial systems, Kenya. *J. African Earth Sci.* **2020**, *163*, 103748. <https://doi.org/10.1016/j.jafrearsci.2019.103748>.
202. Zhang, H.; Xue, L.; Wei, G.; Dong, Z.; Meng, X. Assessing Vegetation Dynamics and Landscape Ecological Risk on the Mainstream of Tarim River, China. *Water* **2020**, *12*, 2156. <https://doi.org/10.3390/w12082156>.
203. Nagler, P.L.; Barreto-Muñoz, A.; Borujeni, S.C.; Nouri, H.; Jarchow, C.J.; Didan, K. Riparian area changes in greenness and water use on the lower Colorado river in the USA from 2000 to 2020. *Remote Sens.* **2021**, *13*, 1332. <https://doi.org/10.3390/rs13071332>.
204. Güneralp, İ.; Filippi, A.M.; Randall, J. Estimation of floodplain aboveground biomass using multispectral remote sensing and nonparametric modeling. *Int. J. Appl. Earth Obs. Geoinf.* **2014**, *33*, 119–126. <https://doi.org/10.1016/j.jag.2014.05.004>.
205. Fernandes, M.R.; Aguiar, F.C.; Martins, M.J.; Rico, N.; Ferreira, M.T.; Correia, A.C. Carbon Stock Estimations in a Mediterranean Riparian Forest: A Case Study Combining Field Data and UAV Imagery. *Forests* **2020**, *11*, 376. <https://doi.org/10.3390/f11040376>.
206. Wang, Y.; Shen, X.; Jiang, M.; Tong, S.; Lu, X. Spatiotemporal change of aboveground biomass and its response to climate change in marshes of the Tibetan Plateau. *Int. J. Appl. Earth Obs. Geoinf.* **2021**, *102*, 102385. <https://doi.org/10.1016/J.JAG.2021.102385>.

207. Shen, X.; Jiang, M.; Lu, X.; Liu, X.; Liu, B.; Zhang, J.; Wang, X.; Tong, S.; Lei, G.; Wang, S.; et al. Aboveground biomass and its spatial distribution pattern of herbaceous marsh vegetation in China. *Sci. China Earth Sci.* **2021**, *64*, 1115–1125. <https://doi.org/10.1007/S11430-020-9778-7>.
208. Silverman, N.L.; Allred, B.W.; Donnelly, J.P.; Chapman, T.B.; Maestas, J.D.; Wheaton, J.M.; White, J.; Naugle, D.E. Low-tech riparian and wet meadow restoration increases vegetation productivity and resilience across semiarid rangelands. *Restor. Ecol.* **2019**, *27*, 269–278. <https://doi.org/10.1111/rec.12869>.
209. Langhammer, J. UAV Monitoring of Stream Restorations. *Hydrology* **2019**, *6*, 29. <https://doi.org/10.3390/hydrology6020029>.
210. Petrakis, R.; van Leeuwen, W.; Villarreal, M.L.; Tashjian, P.; Dello Russo, R.; Scott, C. Historical Analysis of Riparian Vegetation Change in Response to Shifting Management Objectives on the Middle Rio Grande. *Land* **2017**, *6*, 29. <https://doi.org/10.3390/land6020029>.
211. Piedelobo, L.; Taramelli, A.; Schiavon, E.; Valentini, E.; Molina, J.-L.; Nguyen Xuan, A.; González-Aguilera, D. Assessment of Green Infrastructure in Riparian Zones Using Copernicus Programme. *Remote Sens.* **2019**, *11*, 2967. <https://doi.org/10.3390/rs11242967>.
212. Betz, F.; Lauermann, M.; Cyffka, B. Open source riverscapes: Analyzing the corridor of the Naryn River in Kyrgyzstan based on open access data. *Remote Sens.* **2020**, *12*, 2533. <https://doi.org/10.3390/RS12162533>.
213. Wu, J.; Tang, D. The influence of water conveyances on restoration of vegetation to the lower reaches of Tarim River. *Environ. Earth Sci.* **2010**, *59*, 967–975. <https://doi.org/10.1007/s12665-009-0090-9>.
214. Huylenbroeck, L.; Laslier, M.; Dufour, S.; Georges, B.; Lejeune, P.; Michez, A. Using remote sensing to characterize riparian vegetation: A review of available tools and perspectives for managers. *J. Environ. Manage.* **2020**, *267*, 110652. <https://doi.org/10.1016/j.jenvman.2020.110652>.
215. Schmitz, D.; Blank, M.; Ammond, S.; Patten, D.T. Using historic aerial photography and paleohydrologic techniques to assess long-term ecological response to two Montana dam removals. *J. Environ. Manage.* **2009**, *90*, S237–S248. <https://doi.org/10.1016/j.jenvman.2008.07.028>.
216. Wu, X.; Cai, Y. Land cover changes and landscape dynamics assessment in lower reaches of Tarim River in China. *Chinese Geogr. Sci.* **2004**, *14*, 28–33. <https://doi.org/10.1007/s11769-004-0005-3>.
217. Miklín, J.; Hradecký, J. Confluence of the Morava and Dyje Rivers: A century of landscape changes in maps. *J. Maps* **2016**, *12*, 630–638. <https://doi.org/10.1080/17445647.2015.1068714>.
218. Demissie, B.; Nyssen, J.; Billi, P.; Haile, M.; Vaneetvelde, V.; Frankl, A. Land-use/cover changes in relation to stream dynamics in a marginal graben along the northern Ethiopian Rift Valley. *Phys. Geogr.* **2019**, *40*, 71–90. <https://doi.org/10.1080/02723646.2018.1458577>.
219. Basumatary, H.; Devi, H.S.; Borah, S.B.; Das, A.K. Land cover dynamics and their driving factors in a protected floodplain ecosystem. *River Res. Appl.* **2021**, *37*, 627–643. <https://doi.org/10.1002/rra.3775>.
220. Hooke, J.; Chen, H. Evidence of increase in woody vegetation in a river corridor, Northwest England, 1984–2007. *J. Maps* **2016**, *12*, 484–491. <https://doi.org/10.1080/17445647.2015.1044039>.
221. Milani, G.; Volpi, M.; Tonolla, D.; Doering, M.; Robinson, C.; Kneubühler, M.; Schaepman, M. Robust quantification of riverine land cover dynamics by high-resolution remote sensing. *Remote Sens. Environ.* **2018**, *217*, 491–505. <https://doi.org/10.1016/j.rse.2018.08.035>.
222. Gumrukcuoglu, M.; Goodin, D.G.; Martin, C. Landuse change in upper Kansas river floodplain: Following the 1993 flood. *Nat. Hazards* **2010**, *55*, 467–479. <https://doi.org/10.1007/s11069-010-9540-7>.
223. Ceschin, S.; Tombolini, I.; Abati, S.; Zuccarello, V. The effect of river damming on vegetation: Is it always unfavourable? A case study from the River Tiber (Italy). *Environ. Monit. Assess.* **2015**, *187*, 1–12. <https://doi.org/10.1007/s10661-015-4521-7>.
224. Garófano-Gómez, V.; Martínez-Capel, F.; Bertoldi, W.; Gurnell, A.; Estornell, J.; Segura-Beltrán, F. Six decades of changes in the riparian corridor of a mediterranean river: A synthetic analysis based on historical data sources. *Ecohydrology* **2013**, *6*, 536–553. <https://doi.org/10.1002/eco.1330>.
225. Dykaar, B.B. Floodplain Formation and Cottonwood Colonization Patterns on the Willamette River, Oregon, USA. *Environ. Manage.* **2000**, *25*, 87–104. <https://doi.org/10.1007/s002679910007>.
226. Fu, Y.; Dong, Y.; Xie, Y.; Xu, Z.; Wang, L. Impacts of regional groundwater flow and river fluctuation on floodplain wetlands in the middle reach of the Yellow river. *Water* **2020**, *12*, 1922. <https://doi.org/10.3390/w12071922>.
227. Solins, J.P.; Thorne, J.H.; Cadenasso, M.L. Riparian canopy expansion in an urban landscape: Multiple drivers of vegetation change along headwater streams near Sacramento, California. *Landsc. Urban Plan.* **2018**, *172*, 37–46. <https://doi.org/10.1016/j.landurbplan.2017.12.005>.
228. Gurnell, A.M.; Grabowski, R.C. Vegetation-Hydrogeomorphology Interactions in a Low-Energy, Human-Impacted River. *River Res. Appl.* **2016**, *32*, 202–215. <https://doi.org/10.1002/rra.2922>.
229. Parsons, H.; Gilvear, D. Valley floor landscape change following almost 100 years of flood embankment abandonment on a wandering gravel-bed river. *River Res. Appl.* **2002**, *18*, 461–479. <https://doi.org/10.1002/rra.684>.
230. Picco, L.; Comiti, F.; Mao, L.; Tonon, A.; Lenzi, M.A. Medium and short term riparian vegetation, island and channel evolution in response to human pressure in a regulated gravel bed river (Piave River, Italy). *Catena* **2017**, *149*, 760–769. <https://doi.org/10.1016/j.catena.2016.04.005>.

231. Bao, A.; Huang, Y.; Ma, Y.; Guo, H.; Wang, Y. Assessing the effect of EWDP on vegetation restoration by remote sensing in the lower reaches of Tarim River. *Ecol. Indic.* **2017**, *74*, 261–275. <https://doi.org/10.1016/j.ecolind.2016.11.007>.
232. Gaur, T. Dynamics of landscape change in a mountainous river basin: a case study of the Bhagirathi river, western Himalaya. *Appl. Ecol. Environ. Res.* **2019**, *17*, 8271–8289. https://doi.org/10.15666/aeer/1704_82718289.
233. Zhou, T.; Ren, W.; Peng, S.; Liang, L.; Ren, S.; Wu, J. A riverscape transect approach to studying and restoring river systems: A case study from southern China. *Ecol. Eng.* **2014**, *65*, 147–158. <https://doi.org/10.1016/j.ecoleng.2013.08.005>.
234. Miller, J.R.; Schulz, T.T.; Hobbs, N.T.; Wilson, K.R.; Schrupp, D.L.; Baker, W.L. Changes in the landscape structure of a southeastern Wyoming riparian zone following shifts in stream dynamics. *Biol. Conserv.* **1995**, *72*, 371–379. [https://doi.org/10.1016/0006-3207\(94\)00049-V](https://doi.org/10.1016/0006-3207(94)00049-V).
235. Dufour, S.; Rinaldi, M.; Piégay, H.; Michalon, A. How do river dynamics and human influences affect the landscape pattern of fluvial corridors? Lessons from the Magra River, Central–Northern Italy. *Landsc. Urban Plan.* **2015**, *134*, 107–118. <https://doi.org/10.1016/J.LANDURBPLAN.2014.10.007>.
236. Corenblit, D.; Vautier, F.; González, E.; Steiger, J. Formation and dynamics of vegetated fluvial landforms follow the biogeomorphological succession model in a channelized river. *Earth Surf. Process. Landf.* **2020**, *45*, 2020–2035. <https://doi.org/10.1002/esp.4863>.
237. Caponi, F.; Koch, A.; Bertoldi, W.; Vetsch, D.F.; Siviglia, A. When Does Vegetation Establish on Gravel Bars? Observations and Modeling in the Alpine Rhine River. *Front. Environ. Sci.* **2019**, *7*, 124. <https://doi.org/10.3389/fenvs.2019.00124>.
238. Garofano-Gomez, V.; Metz, M.; Egger, G.; Diaz-Redondo, M.; Hortobágyi, B.; Geerling, G.; Corenblit, D.; Steiger, J. Processus de succession végétale et dynamiqueluviale d'un écosystème riverain mobile en zone tempérée: Le bas Allier (France). *Geomorphol. Reli. Process. Environ.* **2017**, *23*, 187–202.
239. Geerling, G.W.; Ragas, A.M.J.; Leuven, R.S.E.W.; van den Berg, J.H.; Breedveld, M.; Liefhebber, D.; Smits, A.J.M. Succession and Rejuvenation in Floodplains along the River Allier (France). *Hydrobiologia* **2006**, *565*, 71–86. <https://doi.org/10.1007/s10750-005-1906-6>.
240. Hervouet, A.; Dunford, R.; Piégay, H.; Belletti, B.; Trémélo, M.-L. Analysis of Post-flood Recruitment Patterns in Braided-Channel Rivers at Multiple Scales Based on an Image Series Collected by Unmanned Aerial Vehicles, Ultra-light Aerial Vehicles, and Satellites. *GIScience Remote Sens.* **2011**, *48*, 50–73. <https://doi.org/10.2747/1548-1603.48.1.50>.
241. Mossa, J.; Chen, Y.-H.; Kondolf, G.M.; Walls, S.P. Channel and vegetation recovery from dredging of a large river in the Gulf coastal plain, USA. *Earth Surf. Process. Landf.* **2020**, *45*, 1926–1944. <https://doi.org/10.1002/esp.4856>.
242. Belletti, B.; Dufour, S.; Piégay, H. What is the Relative Effect of Space and Time to Explain the Braided River Width and Island Patterns at a Regional Scale? *River Res. Appl.* **2015**, *31*, 1–15. <https://doi.org/10.1002/rra.2714>.
243. Harezlak, V.; Geerling, G.W.; Rogers, C.K.; Penning, W.E.; Augustijn, D.C.M.; Hulscher, S.J.M.H. Revealing 35 years of landcover dynamics in floodplains of trained lowland rivers using satellite data. *River Res. Appl.* **2020**, *36*, rra.3633. <https://doi.org/10.1002/rra.3633>.
244. Vautier, F.; Corenblit, D.; Hortobágyi, B.; Fournoux, L.; Steiger, J. Monitoring and reconstructing past biogeomorphic succession within fluvial corridors using stereophotogrammetry. *Earth Surf. Process. Landf.* **2016**, *41*, 1448–1463. <https://doi.org/10.1002/esp.3962>.
245. Kollmann, J.; Vieli, M.; Edwards, P.J.; Tockner, K.; Ward, J.V. Interactions between vegetation development and island formation in the Alpine river Tagliamento. *Appl. Veg. Sci.* **1999**, *2*, 25–36. <https://doi.org/10.2307/1478878>.
246. Bätz, N.; Colombini, P.; Cherubini, P.; Lane, S.N. Groundwater controls on biogeomorphic succession and river channel morphodynamics. *J. Geophys. Res. Earth Surf.* **2016**, *121*, 1763–1785. <https://doi.org/10.1002/2016JF004009>.
247. Aguiar, F.C.; Martins, M.J.; Silva, P.C.; Fernandes, M.R. Riverscapes downstream of hydropower dams: Effects of altered flows and historical land-use change. *Landsc. Urban Plan.* **2016**, *153*, 83–98. <https://doi.org/10.1016/j.landurbplan.2016.04.009>.
248. Corenblit, D.; Steiger, J.; Tabacchi, E. Biogeomorphologic succession dynamics in a Mediterranean river system. *Ecography* **2010**, *33*, 1136–1148. <https://doi.org/10.1111/j.1600-0587.2010.05894.x>.
249. Tonolla, D.; Geilhausen, M.; Doering, M. Seven decades of hydrogeomorphological changes in a near-natural (Sense River) and a hydropower-regulated (Sarine River) pre-Alpine river floodplain in Western Switzerland. *Earth Surf. Process. Landf.* **2021**, *46*, 252–266. <https://doi.org/10.1002/esp.5017>.
250. Asaeda, T.; Sanjaya, K. The effect of the shortage of gravel sediment in midstream river channels on riparian vegetation cover. *River Res. Appl.* **2017**, *33*, 1107–1118. <https://doi.org/10.1002/rra.3166>.
251. Räßle, B.; Piégay, H.; Stella, J.C.; Mercier, D. What drives riparian vegetation encroachment in braided river channels at patch to reach scales? Insights from annual airborne surveys (Drôme River, SE France, 2005–2011). *Ecohydrology* **2017**, *10*, e1886. <https://doi.org/10.1002/eco.1886>.
252. Hudon, C.; Gagnon, P.; Jean, M. Hydrological factors controlling the spread of common reed (*Phragmites australis*) in the St. Lawrence River (Québec, Canada). *Écoscience* **2005**, *12*, 347–357. <https://doi.org/10.2980/i1195-6860-12-3-347.1>.
253. Morgan, B.E.; Bolger, D.T.; Chipman, J.W.; Dietrich, J.T. Lateral and longitudinal distribution of riparian vegetation along an ephemeral river in Namibia using remote sensing techniques. *J. Arid Environ.* **2020**, *181*, 104220. <https://doi.org/10.1016/j.jaridenv.2020.104220>.

254. Peinetti, H.R.; Kalkhan, M.A.; Coughenour, M.B. Long-term changes in willow spatial distribution on the elk winter range of Rocky Mountain National Park (USA). *Landsc. Ecol.* **2002**, *17*, 341–354. <https://doi.org/10.1023/A:1020530710891>.
255. Shafroth, P.B.; Stromberg, J.C.; Patten, D.T. Riparian Vegetation Response to Altered Disturbance and Stress Regimes. *Ecol. Appl.* **2002**, *12*, 107. <https://doi.org/10.2307/3061140>.
256. Hall, R.K.; Watkins, R.L.; Heggem, D.T.; Jones, K.B.; Kaufmann, P.R.; Moore, S.B.; Gregory, S.J.; Watkins, R.L.; Heggem, D.T.; Jones, K.B.; et al. Quantifying structural physical habitat attributes using LIDAR and hyperspectral imagery. *Environ. Monit Assess* **2009**, *159*, 63–83. <https://doi.org/10.1007/s10661-008-0613-y>.
257. Zhu, X.; Yuan, G.; Yi, X.; Du, T. Quantifying the impacts of river hydrology on riparian vegetation spatial structure: Case study in the lower basin of the Tarim River, China. *Ecohydrology* **2017**, *10*, e1887. <https://doi.org/10.1002/eco.1887>.
258. Rodríguez-González, P.M.; Albuquerque, A.; Martínez-Almarza, M.; Díaz-Delgado, R. Long-term monitoring for conservation management: Lessons from a case study integrating remote sensing and field approaches in floodplain forests. *J. Environ. Manage.* **2017**, *202*, 392–402. <https://doi.org/10.1016/j.jenvman.2017.01.067>.
259. Townsend, P. A Quantitative Fuzzy Approach to Assess Mapped Vegetation Classifications for Ecological Applications. *Remote Sens. Environ.* **2000**, *72*, 253–267. [https://doi.org/10.1016/S0034-4257\(99\)00096-6](https://doi.org/10.1016/S0034-4257(99)00096-6).
260. Townsend, P.A.; Walsh, S.J. Remote sensing of forested wetlands: Application of multitemporal and multispectral satellite imagery to determine plant community composition and structure in southeastern USA. *Plant Ecol.* **2001**, *157*, 129–149. <https://doi.org/10.1023/A:1013999513172>.
261. Michez, A.; Piégay, H.; Jonathan, L.; Claessens, H.; Lejeune, P. Mapping of riparian invasive species with supervised classification of Unmanned Aerial System (UAS) imagery. *Int. J. Appl. Earth Obs. Geoinf.* **2016**, *44*, 88–94. <https://doi.org/10.1016/j.jag.2015.06.014>.
262. Kedia, A.C.; Kapos, B.; Liao, S.; Draper, J.; Eddinger, J.; Updike, C.; Frazier, A.E. An Integrated Spectral–Structural Workflow for Invasive Vegetation Mapping in an Arid Region Using Drones. *Drones* **2021**, *5*, 19. <https://doi.org/10.3390/drones5010019>.
263. Bedford, A.; Sankey, T.T.; Sankey, J.B.; Durning, L.; Ralston, B.E. Remote sensing of tamarisk beetle (*Diorhabda carinulata*) impacts along 412 km of the Colorado River in the Grand Canyon, Arizona, USA. *Ecol. Indic.* **2018**, *89*, 365–375. <https://doi.org/10.1016/j.ecolind.2018.02.026>.
264. Caruso, B.S.; Pithie, C.; Edmondson, L. Invasive riparian vegetation response to flow regimes and flood pulses in a braided river floodplain. *J. Environ. Manage.* **2013**, *125*, 156–168. <https://doi.org/10.1016/j.jenvman.2013.03.054>.
265. Caruso, B.S.; Edmondson, L.; Pithie, C. Braided river flow and invasive vegetation dynamics in the southern Alps, New Zealand. *Environ. Manage.* **2013**, *52*, 1–18. <https://doi.org/10.1007/s00267-013-0070-4>.
266. VonBank, J.A.; Casper, A.F.; Yetter, A.P.; Hagy, H.M. Evaluating a Rapid Aerial Survey for Floating-Leaved Aquatic Vegetation. *Wetlands* **2017**, *37*, 753–762. <https://doi.org/10.1007/s13157-017-0910-8>.
267. Husson, E.; Hagner, O.; Ecke, F. Unmanned aircraft systems help to map aquatic vegetation. *Appl. Veg. Sci.* **2014**, *17*, 567–577. <https://doi.org/10.1111/avsc.12072>.
268. Northcott, K.; Andersen, D.C.; Cooper, D.J. The influence of river regulation and land use on floodplain forest regeneration in the semi-arid upper Colorado River Basin, USA. *River Res. Appl.* **2007**, *23*, 565–577. <https://doi.org/10.1002/rra.1007>.
269. Saarinen, N.; Vastaranta, M.; Vaaja, M.; Lotsari, E.; Jaakkola, A.; Kukko, A.; Kaartinen, H.; Holopainen, M.; Hyyppä, H.; Alho, P. Area-Based Approach for Mapping and Monitoring Riverine Vegetation Using Mobile Laser Scanning. *Remote Sens.* **2013**, *5*, 5285–5303. <https://doi.org/10.3390/RS5105285>.
270. Freeman, R.E.; Stanley, E.H.; Turner, M.G. Analysis and conservation implications of landscape change in the wisconsin river floodplain, USA. *Ecol. Appl.* **2003**, *13*, 416–431.
271. Tormos, T.; Kosuth, P.; Durrieu, S.; Villeneuve, B.; Wasson, J.G. Improving the quantification of land cover pressure on stream ecological status at the riparian scale using High Spatial Resolution Imagery. *Phys. Chem. Earth* **2011**, *36*, 549–559. <https://doi.org/10.1016/j.pce.2010.07.012>.
272. Hamilton, S.K.; Kellndorfer, J.; Lehner, B.; Tobler, M. Remote sensing of floodplain geomorphology as a surrogate for biodiversity in a tropical river system (Madre de Dios, Peru). *Geomorphology* **2007**, *89*, 23–38. <https://doi.org/10.1016/j.geomorph.2006.07.024>.
273. Bocchi, S.; La Rosa, D.; Pileri, P. Agro-ecological analysis for the eu water framework directive: An applied case study for the river contract of the Seveso basin (Italy). *Environ. Manage.* **2012**, *50*, 514–529. <https://doi.org/10.1007/s00267-012-9925-3>.
274. Wiens, J.; Sutter, R.; Anderson, M.; Blanchard, J.; Barnett, A.; Aguilar-Amuchastegui, N.; Avery, C.; Laine, S. Selecting and conserving lands for biodiversity: The role of remote sensing. *Remote Sens. Environ.* **2009**, *113*, 1370–1381. <https://doi.org/10.1016/j.rse.2008.06.020>.
275. Martínez-Fernández, V.; González, E.; López-Almansa, J.C.; González, S.M.; García de Jalón, D. Dismantling artificial levees and channel revetments promotes channel widening and regeneration of riparian vegetation over long river segments. *Ecol. Eng.* **2017**, *108*, 132–142. <https://doi.org/10.1016/j.ecoleng.2017.08.005>.
276. Sawtschuk, J.; Delisle, M.; Mesmin, X.; Bernez, I. How past riparian management practices can affect composition and structure of vegetation for headwater ecological restoration projects. *Acta Bot. Gallica: Bot. Lett.* **2014**, *161*, 309–320. <https://doi.org/10.1080/12538078.2014.933362>.

277. González, E.; González-Sanchis, M.; Cabezas, Á.; Comín, F.A.; Muller, E. Recent changes in the riparian forest of a large regulated mediterranean river: Implications for management. *Environ. Manage.* **2010**, *45*, 669–681. <https://doi.org/10.1007/s00267-010-9441-2>.
278. Toda, Y.; Zhou, Y.; Sakai, N. Modeling of riparian vegetation dynamics and its application to sand-bed river. *J. Hydro-Environ. Res.* **2020**, *30*, 3–13. <https://doi.org/10.1016/j.jher.2019.09.003>.
279. Callow, J.N. Understanding patterns of vegetation degradation at meaningful scales within saline landscapes. *Ecohydrology* **2011**, *4*, 841–854. <https://doi.org/10.1002/eco.190>.
280. Han, M.; Brierley, G. Channel geomorphology and riparian vegetation interactions along four anabranching reaches of the Upper Yellow River. *Prog. Phys. Geogr. Earth Environ.* **2020**, *44*, 898–922. <https://doi.org/10.1177/0309133320938768>.
281. Corenblit, D.; Garófano-Gómez, V.; González, E.; Hortobágyi, B.; Julien, F.; Lambs, L.; Otto, T.; Roussel, E.; Steiger, J.; Tabacchi, E.; et al. Niche construction within riparian corridors. Part II: The unexplored role of positive intraspecific interactions in Salicaceae species. *Geomorphology* **2018**, *305*, 112–122. <https://doi.org/10.1016/j.geomorph.2017.09.016>.
282. Lallias-Tacon, S.; Liébault, F.; Piégay, H. Use of airborne LiDAR and historical aerial photos for characterising the history of braided river floodplain morphology and vegetation responses. *CATENA* **2017**, *149*, 742–759. <https://doi.org/10.1016/j.catena.2016.07.038>.
283. Rood, S.B.; Kaluthota, S.; Philipson, L.J.; Slaney, J.; Jones, E.; Chasmer, L.; Hopkinson, C. Camo-maps: An efficient method to assess and project riparian vegetation colonization after a major river flood. *Ecol. Eng.* **2019**, *141*, 105610. <https://doi.org/10.1016/j.ecoleng.2019.105610>.
284. Girel, J.; Garguet-Duport, B.; Pautou, G. Landscape Structure and Historical Processes along Diked European Valleys: A Case Study of the Arc/Isère Confluence (Savoie, France). *Environ. Manage.* **1997**, *21*, 891–907. <https://doi.org/10.1007/s002679900075>.
285. Nagler, P.; Glenn, E.P.; Hursh, K.; Curtis, C.; Huete, A. Vegetation mapping for change detection on an arid-zone river. *Environ. Monit. Assess.* **2005**, *109*, 255–274. <https://doi.org/10.1007/s10661-005-6285-y>.
286. Dakin Kuiper, S.; Coops, N.C.; Tompalski, P.; Hinch, S.G.; Nonis, A.; White, J.C.; Hamilton, J.; Davis, D.J. Characterizing stream morphological features important for fish habitat using airborne laser scanning data. *Remote Sens. Environ.* **2022**, *272*, 112948. <https://doi.org/10.1016/j.rse.2022.112948>.
287. Piégay, H.; Thevenet, A.; Kondolf, G.; Landon, N. Physical and human factors influencing potential fish habitat distribution along a mountain river, France. *Geogr. Ann. Ser. A Phys. Geogr.* **2000**, *82*, 121–136. <https://doi.org/10.1111/j.0435-3676.2000.00117.x>.
288. Whited, D.C.; Kimball, J.S.; Lorang, M.S.; Stanford, J.A. Estimation of juvenile salmon habitat in Pacific rim rivers using multiscalar remote sensing and geospatial analysis. *River Res. Appl.* **2013**, *29*, 135–148. <https://doi.org/10.1002/rra.1585>.
289. Tomlinson, M.J.; Gergel, S.E.; Beechie, T.J.; McClure, M.M. Long-term changes in river–floodplain dynamics: Implications for salmonid habitat in the Interior Columbia Basin, USA. *Ecol. Appl.* **2011**, *21*, 1643–1658. <https://doi.org/10.1890/10-1238.1>.
290. Keller, D.L.; Laub, B.G.; Birdsey, P.; Dean, D.J. Effects of Flooding and Tamarisk Removal on Habitat for Sensitive Fish Species in the San Rafael River, Utah: Implications for Fish Habitat Enhancement and Future Restoration Efforts. *Environ. Manage.* **2014**, *54*, 465–478. <https://doi.org/10.1007/s00267-014-0318-7>.
291. Arantes, C.C.; Winemiller, K.O.; Petrere, M.; Castello, L.; Hess, L.L.; Freitas, C.E.C. Relationships between forest cover and fish diversity in the Amazon River floodplain. *J. Appl. Ecol.* **2018**, *55*, 386–395. <https://doi.org/10.1111/1365-2664.12967>.
292. Mollot, L.A.; Bilby, R.E. The use of geographic information systems, remote sensing, and suitability modeling to identify conifer restoration sites with high biological potential for anadromous fish at the cedar river municipal watershed in Western Washington, U.S.A. *Restor. Ecol.* **2008**, *16*, 336–347. <https://doi.org/10.1111/j.1526-100X.2007.00340.x>.
293. van der Most, M.; Hudson, P.F. The influence of floodplain geomorphology and hydrologic connectivity on alligator gar (*Atractosteus spatula*) habitat along the embanked floodplain of the Lower Mississippi River. *Geomorphology* **2018**, *302*, 62–75. <https://doi.org/10.1016/j.geomorph.2017.09.032>.
294. Villamarín, F.; Marioni, B.; Thorbjarnarson, J.B.; Nelson, B.W.; Botero-Arias, R.; Magnusson, W.E. Conservation and management implications of nest-site selection of the sympatric crocodylians *Melanosuchus niger* and *Caiman crocodylus* in Central Amazonia, Brazil. *Biol. Conserv.* **2011**, *144*, 913–919. <https://doi.org/10.1016/j.biocon.2010.12.012>.
295. Lafage, D.; Secondi, J.; Georges, A.; Bouzillé, J.-B.; Pétilon, J. Satellite-derived vegetation indices as surrogate of species richness and abundance of ground beetles in temperate floodplains. *Insect Conserv. Divers.* **2014**, *7*, 327–333. <https://doi.org/10.1111/ICAD.12056>.
296. Bateman, H.L.; Nagler, P.L.; Glenn, E.P. Plot- and landscape-level changes in climate and vegetation following defoliation of exotic saltcedar (*Tamarix* sp.) from the biocontrol agent *Diorhabda carinulata* along a stream in the Mojave Desert (USA). *J. Arid Environ.* **2013**, *89*, 16–20. <https://doi.org/10.1016/j.jaridenv.2012.09.011>.
297. McFarland, T.M.; Van Riper, C.; Johnson, G.E. Evaluation of NDVI to assess avian abundance and richness along the upper San Pedro River. *J. Arid Environ.* **2012**, *77*, 45–53. <https://doi.org/10.1016/j.jaridenv.2011.09.010>.
298. Surian, N.; Rinaldi, M. Morphological response to river engineering and management in alluvial channels in Italy. *Geomorphology* **2003**, *50*, 307–326. [https://doi.org/10.1016/S0169-555X\(02\)00219-2](https://doi.org/10.1016/S0169-555X(02)00219-2).
299. Kidová, A.; Lehotský, M.; Rusnák, M. Geomorphic diversity in the braided-wandering Belá River, Slovak Carpathians, as a response to flood variability and environmental changes. *Geomorphology* **2016**, *272*, 137–149. <https://doi.org/10.1016/j.geomorph.2016.01.002>.

300. Marchese, E.; Scorpio, V.; Fuller, I.; McColl, S.; Comiti, F. Morphological changes in Alpine rivers following the end of the Little Ice Age. *Geomorphology* **2017**, *295*, 811–826. <https://doi.org/10.1016/j.geomorph.2017.07.018>.
301. Liro, M. Gravel-bed channel changes upstream of a reservoir: The case of the Dunajec River upstream of the Czorsztyn Reservoir, southern Poland. *Geomorphology* **2015**, *228*, 694–702. <https://doi.org/10.1016/j.geomorph.2014.10.030>.
302. Reinhardt, L.; Jerolmack, D.; Cardinale, B.J.; Vanacker, V.; Wright, J. Dynamic interactions of life and its landscape: Feedbacks at the interface of geomorphology and ecology. *Earth Surf. Process. Landf.* **2010**, *35*, 78–101. <https://doi.org/10.1002/esp.1912>.
303. James, M.R.; Chandler, J.H.; Eltner, A.; Fraser, C.; Miller, P.E.; Mills, J.P.; Noble, T.; Robson, S.; Lane, S.N. Guidelines on the use of structure-from-motion photogrammetry in geomorphic research. *Earth Surf. Process. Landf.* **2019**, *44*, 2081–2084. <https://doi.org/10.1002/ESP.4637>.
304. James, M.R.; Robson, S. Mitigating systematic error in topographic models derived from UAV and ground-based image networks. *Earth Surf. Process. Landf.* **2014**, *39*, 1413–1420. <https://doi.org/10.1002/esp.3609>.
305. Sanz-Ablanedo, E.; Chandler, J.H.; Ballesteros-Pérez, P.; Rodríguez-Pérez, J.R. Reducing systematic dome errors in digital elevation models through better UAV flight design. *Earth Surf. Process. Landf.* **2020**, *45*, 2134–2147. <https://doi.org/10.1002/esp.4871>.
306. Piégay, H.; Arnaud, F.; Belletti, B.; Bertrand, M.; Bizzi, S.; Carbonneau, P.; Dufour, S.; Liébault, F.; Ruiz-Villanueva, V.; Slater, L. Remotely sensed rivers in the Anthropocene: State of the art and prospects. *Earth Surf. Process. Landf.* **2020**, *45*, 157–188. <https://doi.org/10.1002/esp.4787>.
307. Roux, C.; Alber, A.; Bertrand, M.; Vaudor, L.; Piégay, H. “FluvialCorridor”: A new ArcGIS toolbox package for multiscale riverscape exploration. *Geomorphology* **2015**, *242*, 29–37. <https://doi.org/10.1016/j.geomorph.2014.04.018>.
308. Mckean, J.; Nagel, D.; Tonina, D.; Bailey, P.; Wright, C.W.; Bohn, C.; Nayegandhi, A. Remote Sensing Remote Sensing of Channels and Riparian Zones with a Narrow-Beam Aquatic-Terrestrial LIDAR. *Remote Sens* **2009**, *1*, 1065–1096. <https://doi.org/10.3390/rs1041065>.
309. Wheaton, J.M.; Brasington, J.; Darby, S.E.; Sear, D.A. Accounting for uncertainty in DEMs from repeat topographic surveys: Improved sediment budgets. *Earth Surf. Process. Landf.* **2009**, *35*, 136–156. <https://doi.org/10.1002/esp.1886>.
310. Piégay, H.; Chabot, A.; Le Lay, Y.-F. Some comments about resilience: From cyclicity to trajectory, a shift in living and nonliving system theory. *Geomorphology* **2018**, *367*, 106527. <https://doi.org/10.1016/J.GEOMORPH.2018.09.018>.
311. Eltner, A.; Bressan, P.O.; Akiyama, T.; Gonçalves, W.N.; Marcato Junior, J. Using Deep Learning for Automatic Water Stage Measurements. *Water Resour. Res.* **2021**, *57*, e2020WR027608. <https://doi.org/10.1029/2020WR027608>.